DESIGN STUDIES OF A CLASS OF MULTIVARIABLE FEEDBACK CONTROL SYSTEMS

by

CHARLES ROBERT BAIRD

B.E., Nova Scotia Technical College, 1957

A THESIS SUBMITTED IN PARTIAL FULFILMENT OF THE REQUIREMENTS FOR THE DEGREE OF

MASTER OF APPLIED SCIENCE

In the Department of

Electrical Engineering

We accept this thesis as conforming to the required standard

Members of the Department
of Electrical Engineering

The University of British Columbia

September 1962

In presenting this thesis in partial fulfilment of the requirements for an advanced degree at the University of British Columbia, I agree that the Library shall make it freely available for reference and study. I further agree that permission for extensive copying of this thesis for scholarly purposes may be granted by the Head of my Department or by his representatives. It is understood that copying or publication of this thesis for financial gain shall not be allowed without my written permission.

Department of Electrical Engineering

The University of British Columbia,
Vancouver 8, Canada.

Date Oct. 4, 1962

ABSTRACT

Methods of designing multivariable feedback control systems based on system eigenvalues and matrix diagonalization are discussed. It is shown that these methods allow single-variable graphical analysis and design techniques to be applied to multivariable systems. The experimental determination of system eigenvalues is shown to be feasible. The suitability of these methods in conjunction with simulation studies for investigation and design purposes is also shown.

A simulated two-axis tracking system is used to compare the eigenvalue method and the diagonalized method.

The eigenvalue method is applied to a system of four parallel-operated synchronous machines and graphical methods of stability investigation are discussed.

ACKNOWLEDGEMENT

The author would like to thank the supervising professor of this project, Dr. E.V. Bohn, for his help and guidance during the course of this research.

The author is indebted to the British Columbia Electric Company Limited for a scholarship awarded in 1960 and to the National Research Council for additional support from the Block Term Grant (BT-68) in the form of a Research Assistantship.

TABLE OF CONTENTS

LIST OF ILLUSTRATIONS

page

LIST OF TABLES

DESIGN STUDIES OF A CLASS OF MULTIVARIABLE FEEDBACK CONTROL SYSTEMS

1. INTRODUCTION

In the design of conventional single-variable linear feedback control systems Nyquist and root-locus diagrams are of considerable practical use. These graphical methods are based on the complex frequency response and enable the designer to choose a suitable system configuration and to study the effect of parameter variations. A suitable choice of system configuration and parameter values can then be made based on engineering experience or a simulated study of the system.

An analytic design approach to a complete system synthesis is possible if suitable criteria for optimum response are formulated analytically. The two most suitable and therefore most often used criteria are the minimization of mean-square error and the specification of closed-loop response.

Both the analytical and the graphical methods have been applied to the design and synthesis of multivariable control systems.

A multivariable control system is one with n independent inputs and m dependent outputs where n and m

are integers and

$$n > 1$$

$$m \geq 1$$

Consider Figure 1 which represents a linear multivariable feedback control system and let n = m.

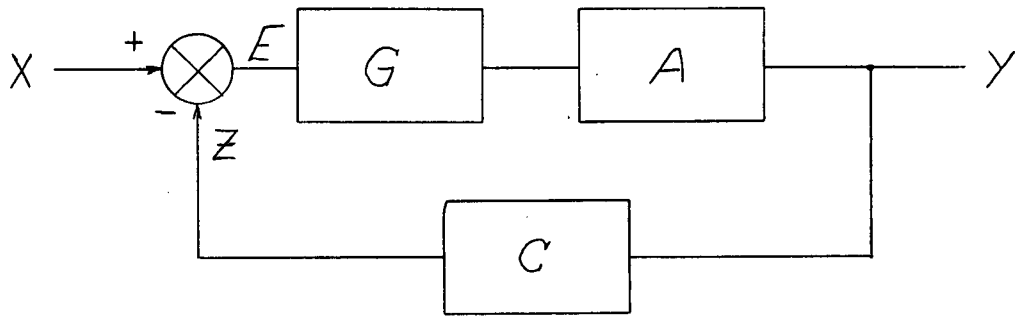

Figure 1-1. A Linear Multivariable Feedback Control System

X and Y are column matrices whose elements are the Laplace transforms of the input and output signals respectively.

$$X = \begin{pmatrix} X_1(s) \\ \vdots \\ X_n(s) \end{pmatrix} \qquad Y = \begin{pmatrix} Y_1(s) \\ \vdots \\ Y_n(s) \end{pmatrix}$$

and

$$G = \begin{pmatrix} G_{11}(s) & \cdots & G_{1n}(s) \\ \vdots & & \vdots \\ G_{n1}(s) & \cdots & G_{nn}(s) \end{pmatrix}$$

$$A = \begin{pmatrix} A_{11}(s) & \cdots & A_{1n}(s) \\ \vdots & & \vdots \\ A_{n1}(s) & \cdots & A_{nn}(s) \end{pmatrix}$$

$$C = \begin{pmatrix} C_{11}(s) & \cdots & C_{1n}(s) \\ \vdots & & \vdots \\ C_{n1}(s) & \cdots & C_{nn}(s) \end{pmatrix}$$

are transfer matrices.

Analysis of the system of Figure 1-1 gives the following equations:

$$AGE = Y \qquad \ldots(1\text{-}1)$$

$$E = X - Z \qquad \ldots(1\text{-}2)$$

$$= X - CY \qquad \ldots(1\text{-}3)$$

Thus $$AG(X - CY) = Y \qquad \ldots(1\text{-}4)$$

or $$AGX = (AGC + I)Y \qquad \ldots(1\text{-}5)$$

where I is the unit matrix.

Also $$Y = (I + AGC)^{-1}AGX \qquad \ldots(1\text{-}6)$$

provided (I + AGC) is nonsingular.

The transfer matrix AGC will be defined as the open-loop transfer matrix and

$$H = (AGC + I)^{-1}AG \qquad \ldots(1\text{-}7)$$

will be defined as the closed-loop transfer matrix.

The poles of the closed-loop transfer matrix are determined by the conditions

$$X = 0$$

$$Y \neq 0 \qquad \ldots(1\text{-}8)$$

which, from equation 1-5, can only be satisfied if the determinant

$$\left|AGC + I\right| = 0 \qquad \ldots(1\text{-}9)$$

Equation 1-9 is known as the characteristic equation. If the system is to be stable, the values of s which satisfy equation 1-9 should all lie in the left-half s-plane.

Povisil and Fuchs[1] have developed a synthesis method which considers the coefficients of the characteristic equation as fixed. This, of course, specifies the poles of the closed-loop transfer matrix and the synthesis deals with the realization of the poles by suitable cross-coupling and feedback connections. Kavanagh[2] and Freeman[3] both assume that a specified H is given and then realize this H by means of a physically realizable compensating matrix. Horowitz[4] considers the design problem from much the same point of view as the above two authors,[2,3] i.e., the desired system response is known. He also discusses at some length the response variations due to changes in the system configuration and also due to

system parameter variations. However, in most practical applications H is not a priori known and these methods are then not applicable.

Hsieh and Leondes[5] discuss the application of the mean-square error criterion, an extension of the Wiener method of synthesis, to multivariable systems. However, analytical methods based on minimizing the mean-square error are not applicable if the statistical properties of the input and the disturbance signals are inadequately known. Even if such information is available, the problem may very well prove to be mathematically intractable. Under these conditions a graphical approach may be more suitable.

Krasovskii[6] and Newman[7] discuss the application of the conventional Nyquist criterion to a two-dimensional system. Bohn[8,9] introduces a procedure for applying known single-variable feedback control system stabilization techniques to a special class of multivariable systems.

In actual design, simulation of the system is, in general, essential. Optimization is then performed on the simulated system by experimental evaluation of the minimum mean-square error, system sensitivity to parameter variations and non-linear effects, or any other suitable criterion.

This study will deal with graphical analysis and design methods and their experimental verification. The

mean-square error will be investigated experimentally. The systems studied will be restricted to a configuration such as that shown in Figure 1-1.

The study basically deals with linear two-variable feedback control systems for two main reasons:

(1) Many such systems occur in practice.

(2) Relative ease of simulation to afford experimental verification of theoretically predicted results.

2. THE EIGENVALUE METHOD OF ANALYSIS AND DESIGN

Consider once more the system shown in Figure 1-1. Suppose now that the elements of the G matrix have the common factor $G_c(s)$. A new matrix can then be defined by

$$G = G_c(s)G' \qquad \ldots(2\text{-}1)$$

Substituting this into equation (1-9) and replacing $G_c(s)$ by $\frac{-1}{\lambda}$ yields

$$\left|AG'C - \lambda I\right| = 0 \qquad \ldots(2\text{-}2)$$

The values of λ which satisfy this equation are the eigenvalues of the transfer matrix AG'C. $G_c(s)$, or $\frac{-1}{\lambda}$, represents the common factor which can be considered as a variable element while all other elements and the system configuration are essentially fixed.

The stability of the system can be determined by an application of the Nyquist criterion. Let

$$\lambda_k(s); \quad k = 1,2,\ldots,n$$

be the eigenvalues of the AG'C matrix. It follows from equation (1-5) that the roots of equation (2-2) are the poles of the closed-loop transfer matrix. The system is stable if there are no values of s in the right half s-plane which are roots of equation (2-2). To determine if this is the case, consider the function $R_k(s)$ defined by

$$R_k(s) = \frac{1}{\lambda_k(s)} + G_c(s) \qquad \ldots(2\text{-}3)$$

From equations (2-2) and (2-3) it is easily seen that the roots of equation (2-2), when $\lambda = \lambda_k$, are the zeros of $R_k(s)$.

The condition for stability is that the zeros of $R_k(s)$ must all lie in the left-half s-plane, i.e., they must all have negative real parts. This can be determined by considering the Nyquist plot of $R_k(s)$ and application of the general condition for stability

$$N = Z - P$$

where P is the number of poles and Z the number of zeros of $R_k(s)$ in the right-half s-plane respectively and N is the number of positive revolutions of the radius vector $R_k(j\omega)$. If $Z = 0$, the system is stable. If $Z > 0$, there are values of s in the right-half s-plane which are roots of equation (2-2) and the system is unstable.

Equation (2-2) can be expressed as a polynomial in λ and may be written in the factored form

$$(\lambda_1 - \lambda)(\lambda_2 - \lambda) \ldots (\lambda_n - \lambda) = 0 \qquad \ldots(2\text{-}4)$$

or

$$\left|\frac{R_1\lambda_1}{G_c}\right|\left|\frac{R_2\lambda_2}{G_c}\right| \ldots \left|\frac{R_n\lambda_n}{G_c}\right| = \frac{1}{G_c^n} \prod_{k=1}^{n} R_k\lambda_k = 0 \qquad \ldots(2\text{-}5)$$

The multivariable system can be considered to be reduced to n equivalent single-variable systems represented by the factors of equation (2-4).

The eigenvalue method essentially considers the system interaction as an entity distinct from the variable element. λ_k may be called an interaction parameter and represents the effect that the system has on the equivalent single-loop system shown in Figure 2-1.

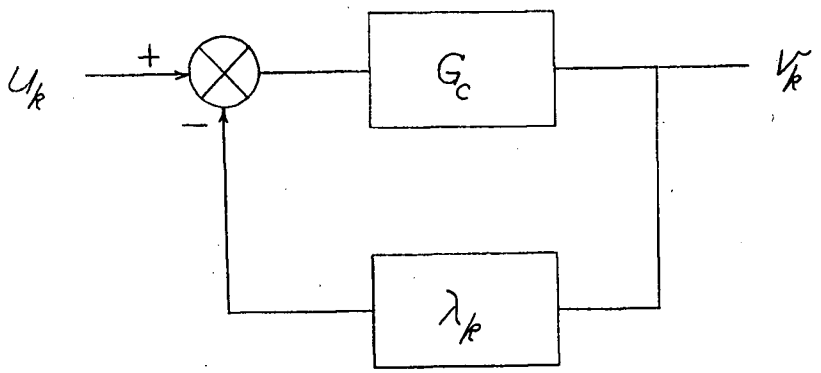

Figure 2-1. Equivalent Single-Loop System

Analysis of the system of Figure 2-1 yields

$$v_k = \frac{G_c}{1 + G_c\lambda_k} u_k \qquad \ldots(2\text{-}6)$$

or

$$v_k = \frac{G_c}{\lambda_k R_k} u_k \qquad \ldots(2\text{-}7)$$

In a conventional single-variable system ($\lambda_k = 1$) we consider a stability vector

$$R = 1 + G_c$$

and the condition $N = Z - P$

If $P = 0$, $N = Z = 0$ for stability (see page 8).

In the eigenvalue system of Figure 2-1 we consider the stability vector as defined by equation (2-3).

$$R_k(s) = \frac{1}{\lambda_k(s)} + G_c(s) \qquad \ldots(2\text{-}8)$$

If $\lambda_k(s)$ is a constant, $\frac{-1}{\lambda_k(s)}$ is a critical point and is considered the same as the -1 point in a conventional

single-variable case. However, if $\lambda_k(s)$ is a function of s, $\frac{-1}{\lambda_k(j\omega)}$ is a critical locus and considerable care must be exercised to determine N.

The above discussion illustrates the application of the Nyquist criterion to multivariable systems where eigenvalues can be introduced.

Another method of investigating system stability is to consider the phase and gain margins by using the Bode Plot Technique to obtain the Nichols plot of the functions $\frac{-1}{\lambda_k(j\omega)}$ and $G_c(j\omega)$. The condition for oscillation is

$$R_k(j\omega) = G_c(j\omega) + \frac{1}{\lambda_k(j\omega)} = 0$$

This requires the magnitude condition

$$\left|G_c(j\omega)\right| = \left|\frac{1}{\lambda_k(j\omega)}\right|$$

and the phase condition

$$\arg.\ G_c(j\omega) = \arg.\ \frac{-1}{\lambda_k(j\omega)}$$

The gain margin is illustrated in Figure 2-2a and the phase margin is illustrated in Figure 2-2b. Figure 2-3 illustrates the phase and gain margins in a Nichols plot of the functions $\frac{-1}{\lambda_k(j\omega)}$ and $G_c(j\omega)$.

The above discussion shows how gain and phase margin criterion may be applied to multivariable systems where eigenvalues can be used.

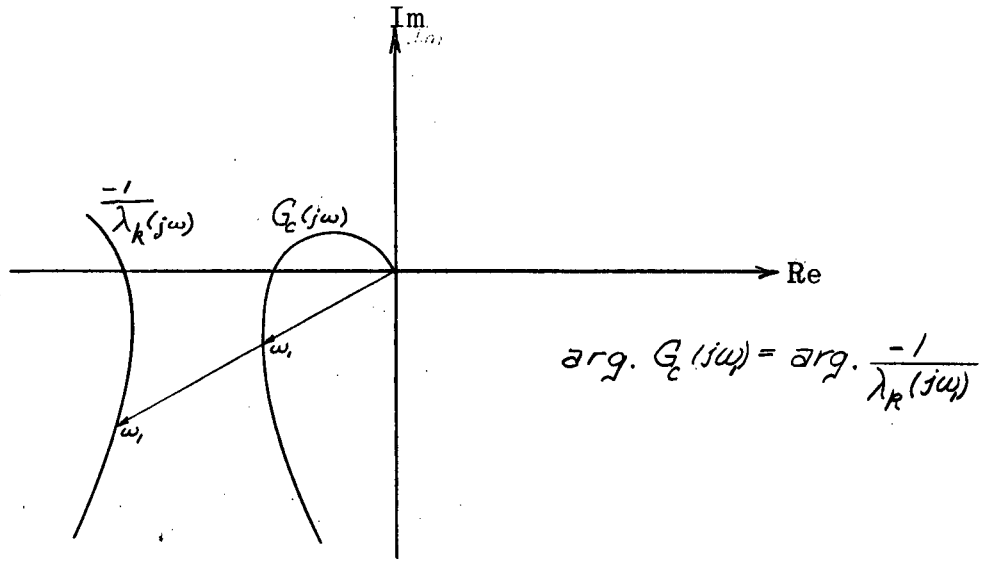

Figure 2-2a Gain Margin $m = 20 \log_{10} \left(\lambda_k(j\omega_1) G_c(j\omega_1) \right)$

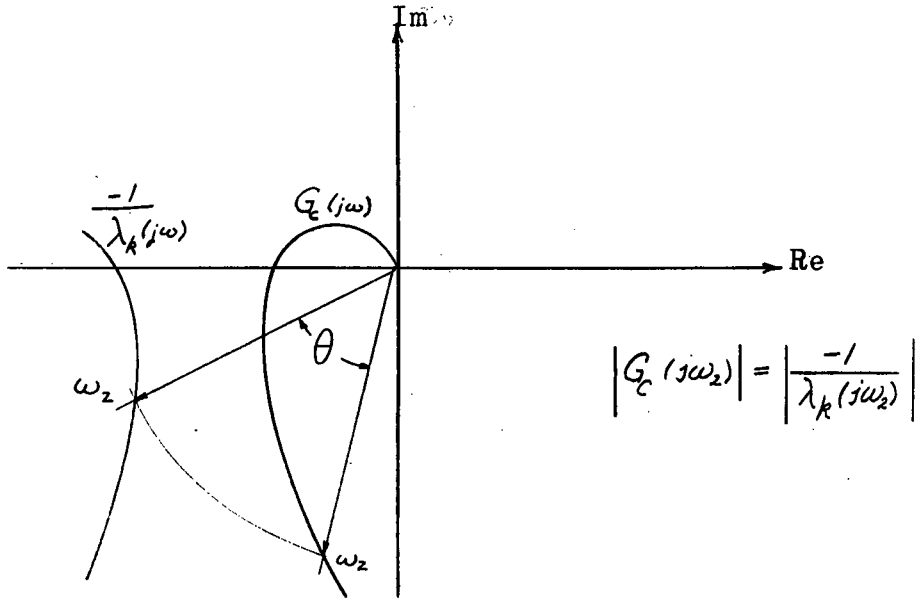

Figure 2-2b Phase Margin $\theta = \arg. G_c(j\omega_2) - \arg. \frac{-1}{\lambda_k(j\omega_2)}$

Using similar reasoning, the eigenvalue method may be used to make other single-variable techniques, such as root-locus plots, applicable to multivariable systems.

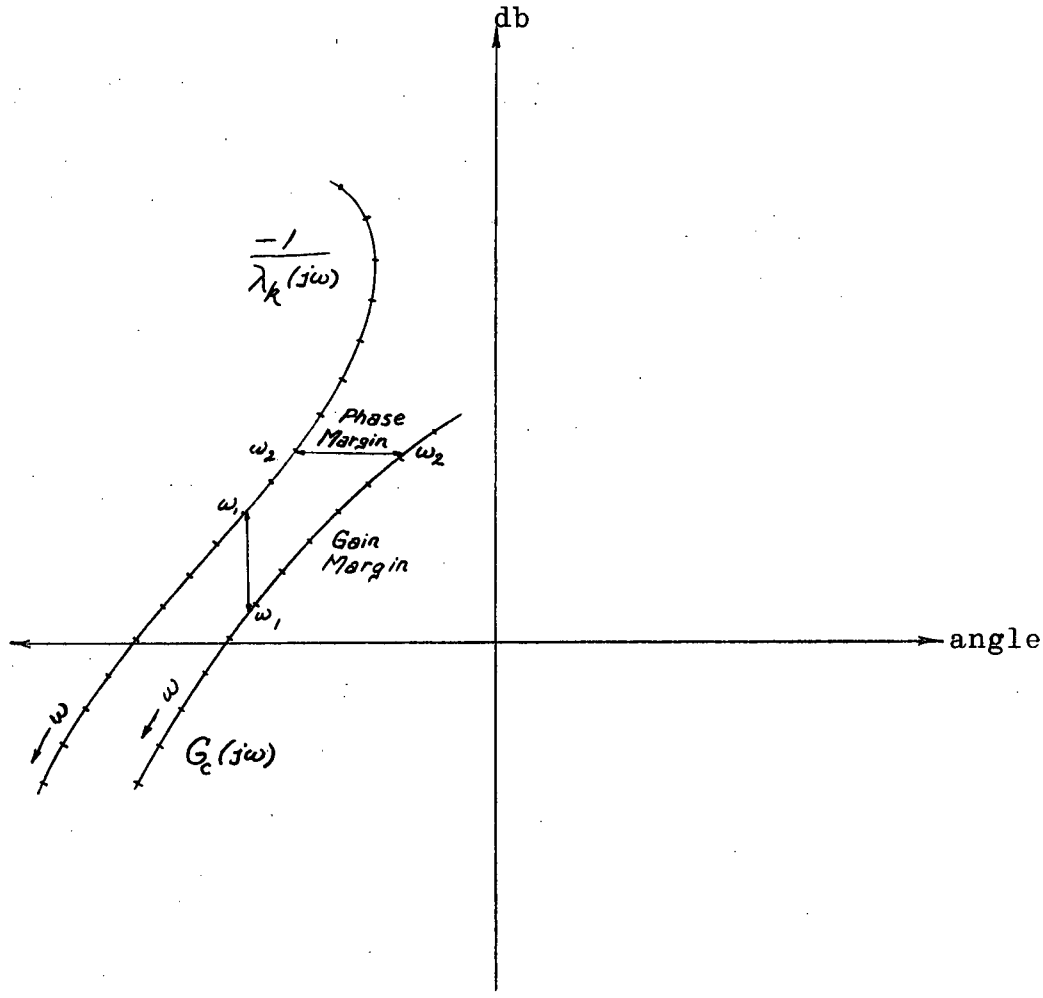

Figure 2-3. Nichols Plot by Bode Plot Technique

2.1 Illustrative Example 2.1

As an illustrative example, consider the system shown in Figure 2-4.

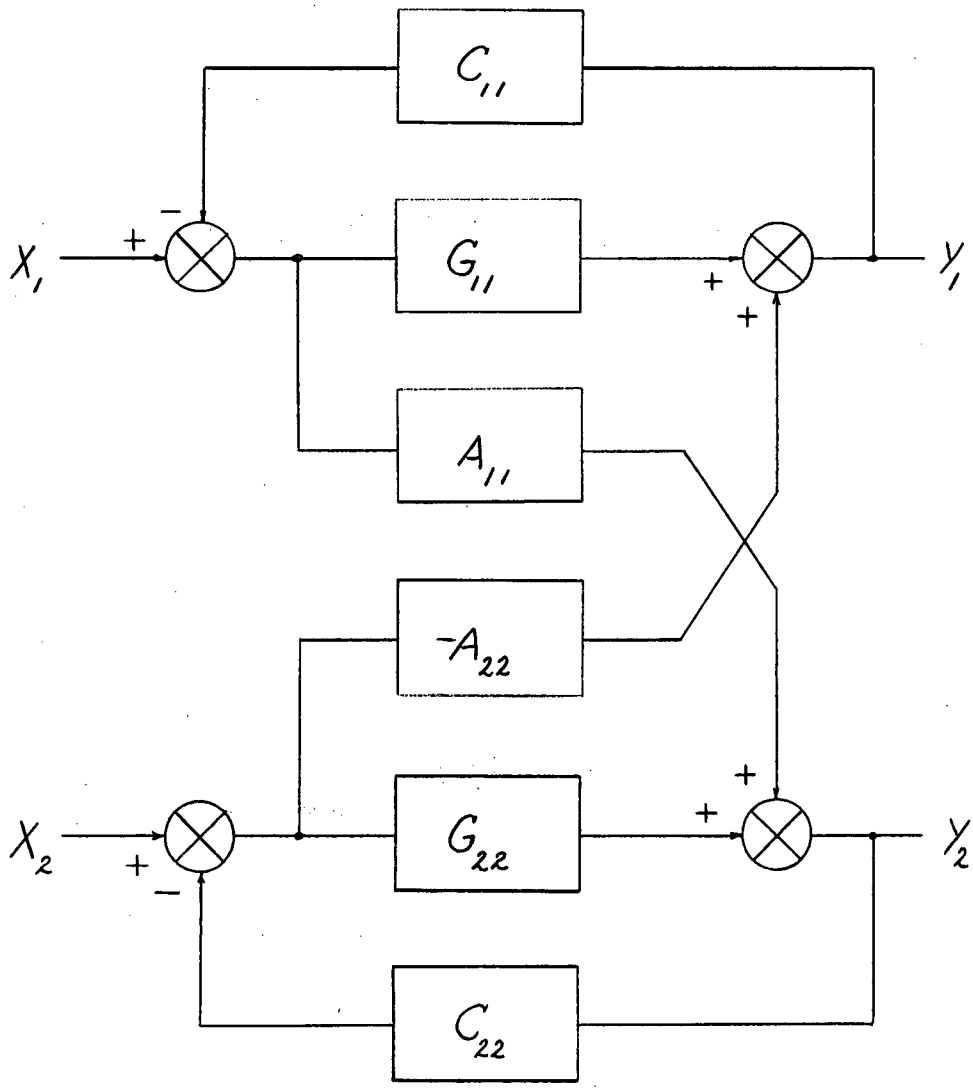

Figure 2-4. Illustrative Example 2.1

Analysis of the system of Figure 2-4 yields

$$G_{11}(X_1 - C_{11}Y_1) - A_{22}(X_2 - C_{22}Y_2) = Y_1$$
$$G_{22}(X_2 - C_{22}Y_2) + A_{11}(X_1 - C_{11}Y_1) = Y_2 \qquad \ldots(2\text{-}8)$$

In matrix form equations (2-8) become

$$\begin{pmatrix} G_{11} & -A_{22} \\ A_{11} & G_{22} \end{pmatrix} \begin{pmatrix} X_1 \\ X_2 \end{pmatrix} = \left[\begin{pmatrix} G_{11}C_{11} & -A_{22}C_{22} \\ A_{11}C_{11} & G_{22}C_{22} \end{pmatrix} + \begin{pmatrix} 1 & 0 \\ 0 & 1 \end{pmatrix} \right] \begin{pmatrix} Y_1 \\ Y_2 \end{pmatrix} \qquad \ldots(2\text{-}9)$$

The characteristic equation is

$$\left| \begin{pmatrix} G_{11}C_{11} & -A_{22}C_{22} \\ A_{11}C_{11} & G_{22}C_{22} \end{pmatrix} + \begin{pmatrix} 1 & 0 \\ 0 & 1 \end{pmatrix} \right| = 0 \qquad \ldots(2\text{-}10)$$

The system shown in Figure 2-4 can be put into the form shown in Figure 2-5.

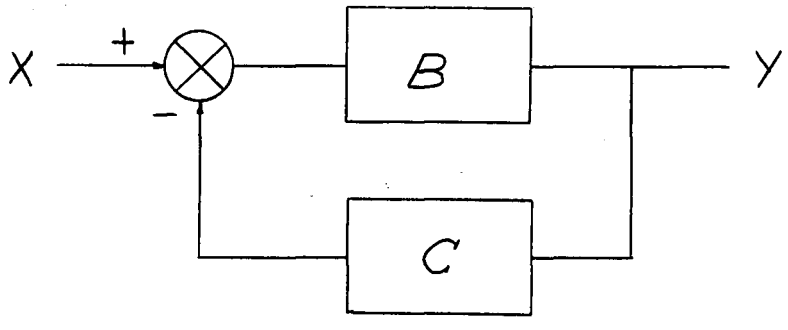

Figure 2-5. Matrix Representation of Figure 2-4

To determine B and C consider the equation

$$BX = (BC + I)Y \qquad \ldots(2\text{-}11)$$

Comparing equations (2-9) and (2-11) yields

$$B = \begin{pmatrix} G_{11} & -A_{22} \\ A_{11} & G_{22} \end{pmatrix} \qquad \ldots(2\text{-}12)$$

$$C = \begin{pmatrix} C_{11} & 0 \\ 0 & C_{22} \end{pmatrix} \qquad \ldots(2\text{-}13)$$

As an example, consider now the case where

$$C_{11} = C_{22} = 1$$

$$G_{11} = G_{22} = G_c(s)$$

$$A_{11} = A_{22} = aG_c(s)$$

$$G_c(s) = \frac{K}{(1 + sT_1)(1 + sT_2)}$$

Therefore, from equation (2-12)

$$B = G_c(s)B' = G_c(s) \begin{pmatrix} 1 & -a \\ a & 1 \end{pmatrix} \qquad \ldots(2\text{-}14)$$

Substituting this into equation (2-11) yields

$$\left| B' + \frac{1}{G_c(s)} I \right| = 0 \qquad \ldots(2\text{-}15)$$

or, if $\frac{1}{G_c(s)}$ is replaced by $-\lambda$,

$$\left| B' - \lambda I \right| = 0 \qquad \ldots(2\text{-}16)$$

This is the eigenvalue equation and it has the form

$$\begin{vmatrix} 1 - \lambda & -a \\ a & 1 - \lambda \end{vmatrix} = 0$$

Solving this equation for the eigenvalues yields

$$\lambda_{1,2} = 1 \pm ja$$

$\frac{-1}{\lambda_1}$ and $\frac{-1}{\lambda_2}$ represent the critical loci. To discuss system stability, we can sketch the Nyquist plot of the functions

$$R_1(s) = \frac{1}{\lambda_1(s)} + G_c(s)$$

$$R_2(s) = \frac{1}{\lambda_2(s)} + G_c(s)$$

as shown in Figure 2-6. If the gain K of the G_c element is increased until the $G_c(j\omega)$ locus intersects the $\frac{-1}{\lambda_2}$ point, i.e., $R_2(j\omega) = 0$, the system becomes unstable.

Figure 2-7 illustrates the Nichols plot of $\frac{-1}{\lambda_k(j\omega)}$ and $G_c(j\omega)$. If the gain K of the G_c element is increased until the gain and phase margins are zero, the system becomes unstable.

2.2 Illustrative Example 2.2

As a further example, suppose that

$$G_{11} = G_{22} = G_c \frac{-K_2}{1 + sT_3}$$

where G_c is considered to be the variable element. Solving the eigenvalue equation (2-16) yields

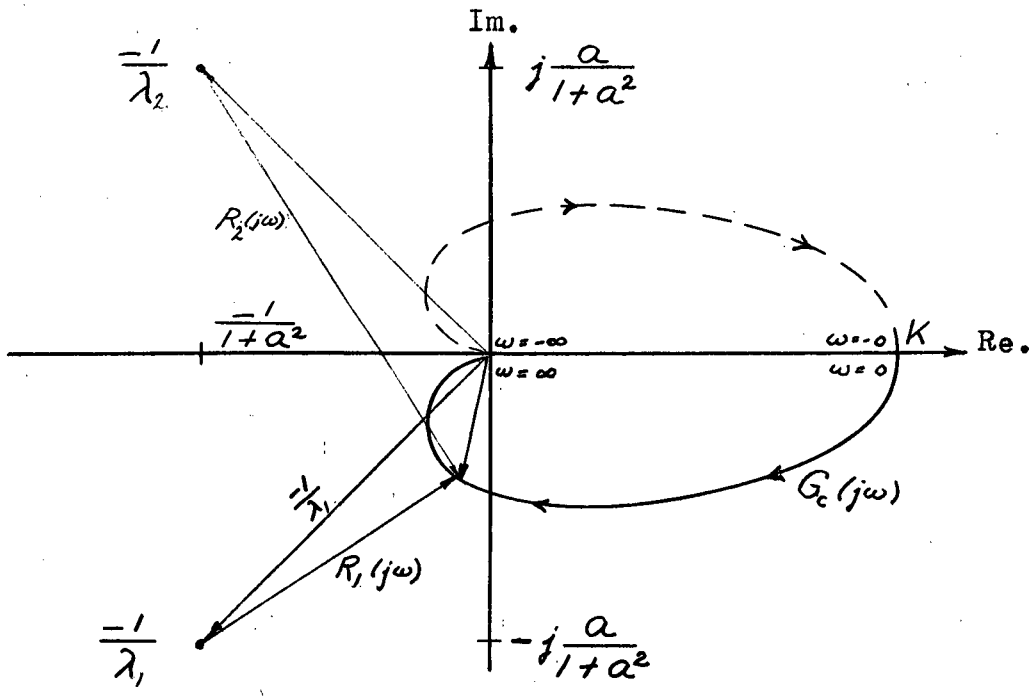

Figure 2-6. Nyquist Plot of $\frac{-1}{\lambda_k(j\omega)}$ and $G_c(j\omega)$.

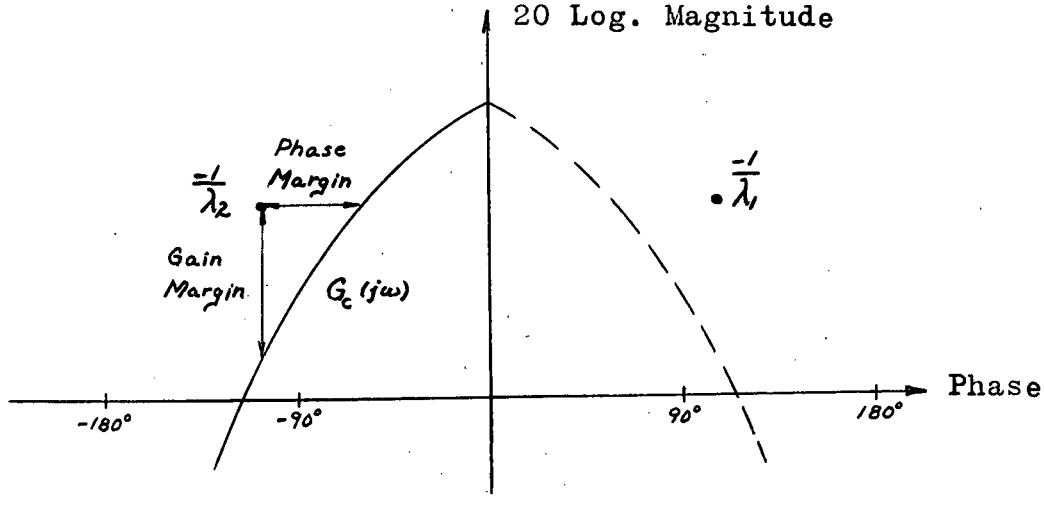

Figure 2-7. Nichols Plot of $\frac{-1}{\lambda_k(j\omega)}$ and $G_c(j\omega)$.

$$\lambda_1 = \frac{-K_2}{1 + sT_3} + ja$$

$$\lambda_2 = \frac{-K_2}{1 + sT_s} - ja$$

The Nyquist plots of $R_1(j\omega)$ and $R_2(j\omega)$ are shown in Figure 2-8. If the gain K of the G_c element is increased until the radius vector $R_1(j\omega) = 0$ (or $R_2(j\omega) = 0$), the system becomes unstable.

Figure 2-9 illustrates the Nichols plot of the functions $\frac{-1}{\lambda_k(j\omega)}$ and $G_c(j\omega)$. If the gain K of the G_c element is increased until the phase and gain margins become zero, the system becomes unstable.

2.3 Illustrative Example 2.3

As a third example, suppose that in equations (2-12) and (2-13);

$$G_{11} = G_{22} = G_c(s) = \frac{K}{(1 + sT_1)(1 + sT_2)}$$

$$A_{11} = A_{22} = a$$

$$C_{11} = C_{22} = 1$$

It follows from equation (2-11) that the characteristic equation is

$$\begin{vmatrix} G_c + 1 & -a \\ a & G_c + 1 \end{vmatrix} = 0$$

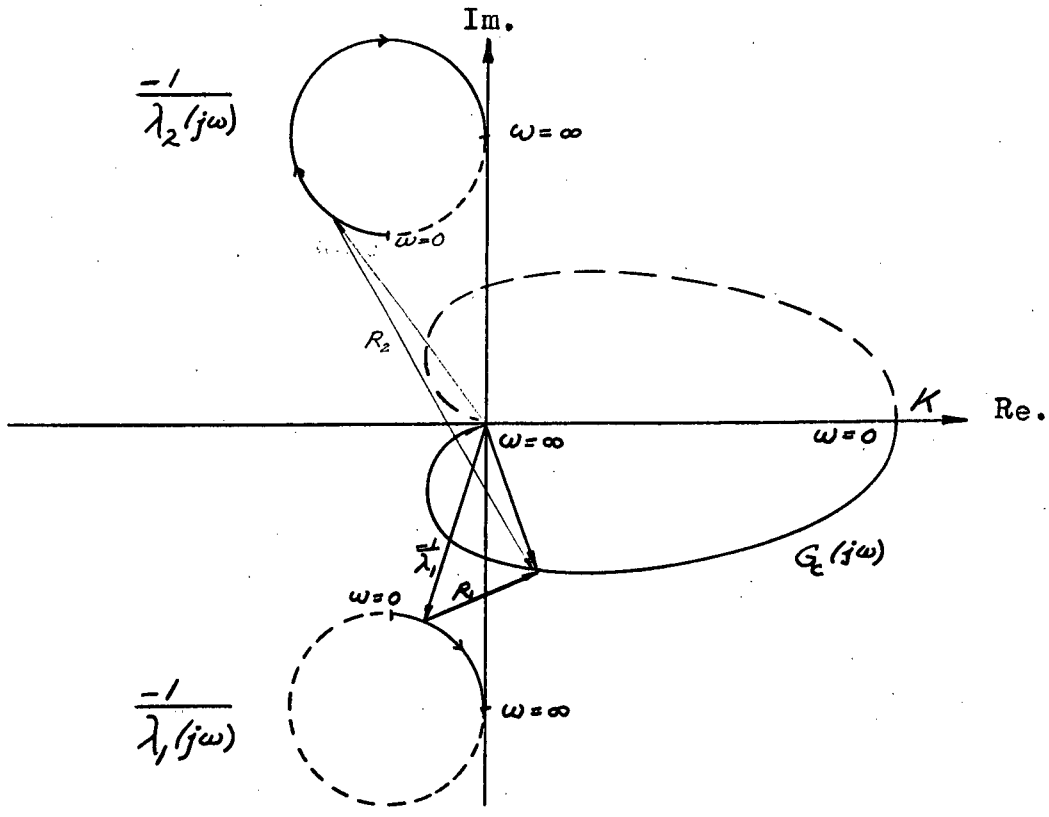

Figure 2-8. Nyquist Plot of $\frac{-1}{\lambda_k(j\omega)}$ and $G_c(j\omega)$.

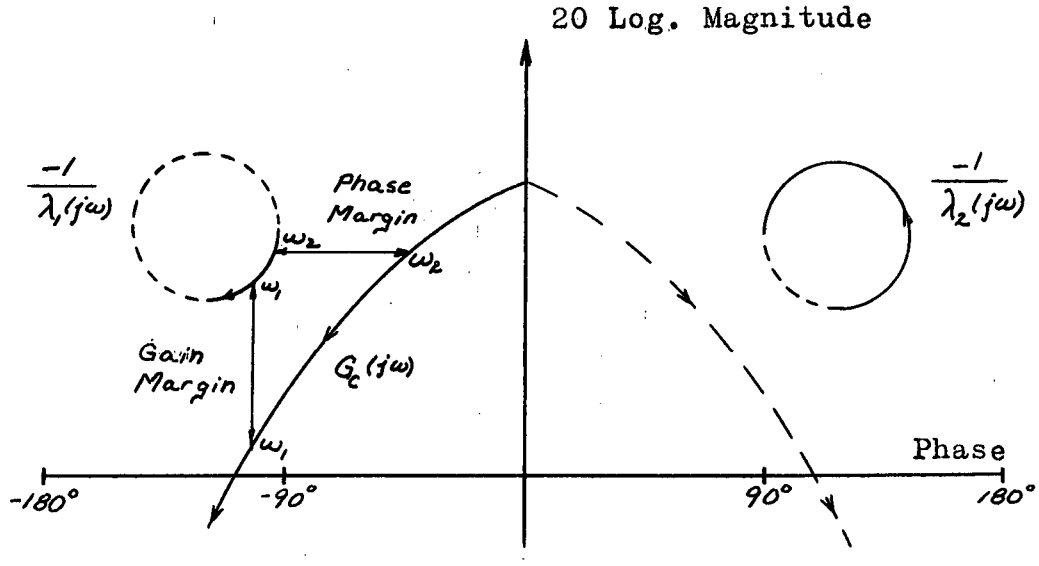

Figure 2-9. Nichols Plot of $\frac{-1}{\lambda_k(j\omega)}$ and $G_c(j\omega)$.

The eigenvalue notation can be introduced by replacing G_c with λ. Carrying out this substitution and solving for the eigenvalues yields

$$(\lambda + 1)^2 + a^2 = 0$$

$$\lambda_{1,2} = -1 \pm ja$$

To determine stability, we consider the Nyquist plot of the function

$$R_k(s) = -\lambda_k(s) + G_c(s) \qquad \ldots(2\text{-}17)$$

which is shown in Figure 2-10. If the radius vector $R_2 = 0$, the system becomes unstable.

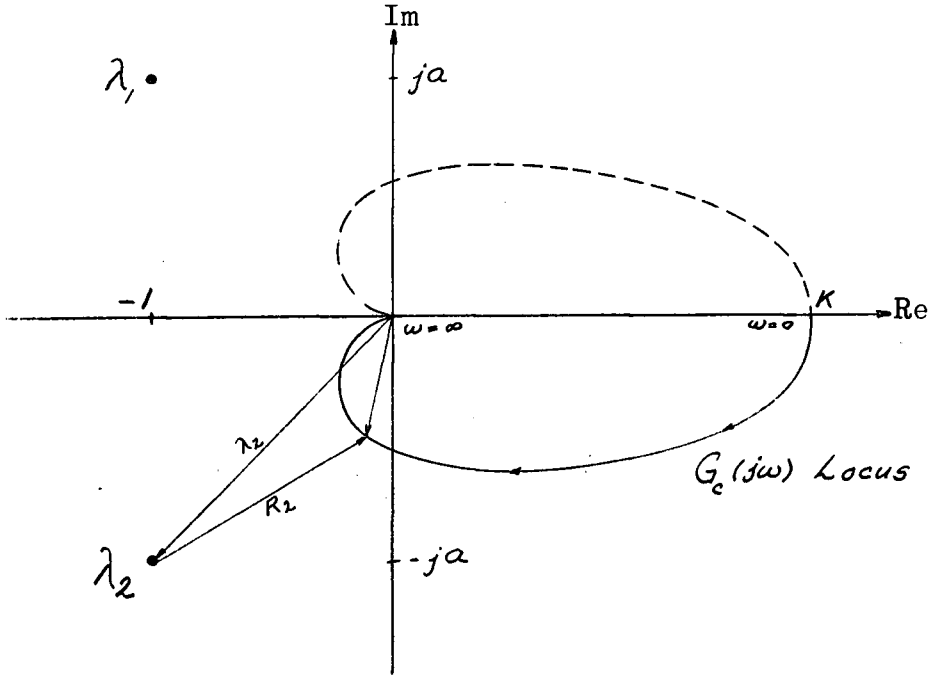

Figure 2-10. Nyquist Plot of $-\lambda_k(j\omega)$ and $G_c(j\omega)$

The following two test examples compare the results of simulation studies on an analog computer with the theoretically predicted results.

2.4 Test Example 2.1

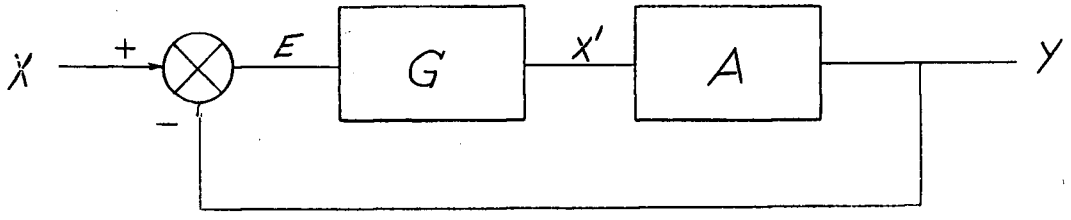

Figure 2-11. Matrix Form of Test Example 2.1

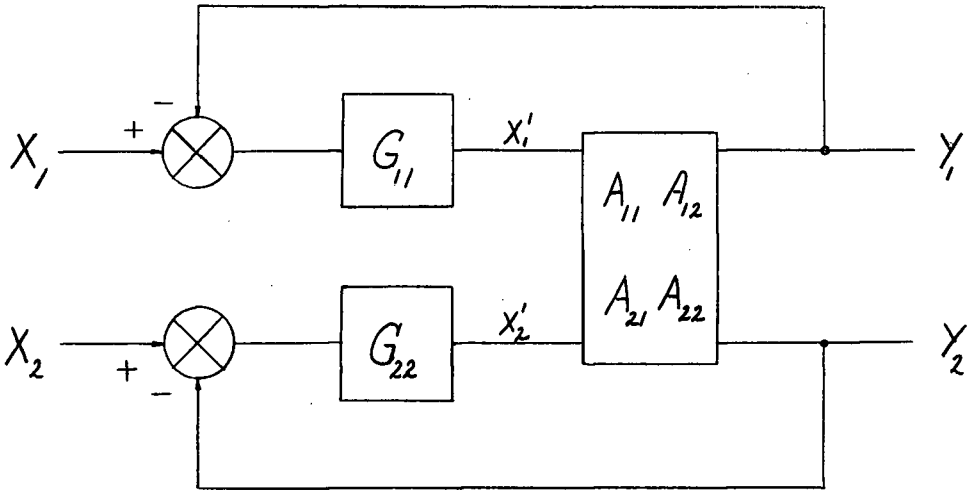

Figure 2-12. Circuit Form of Test Example 2.1

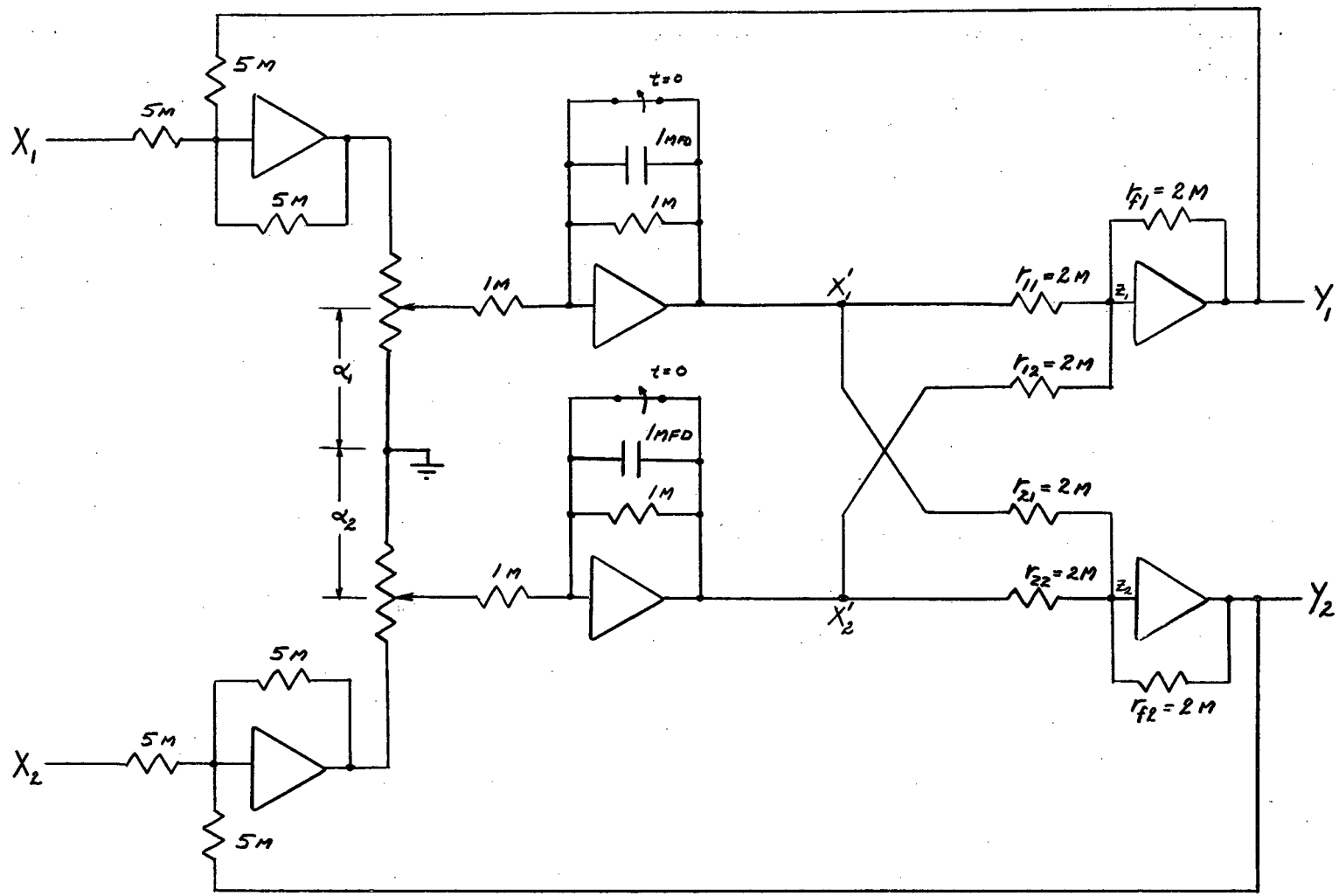

Figure 2-13. Computer Simulation of Test Example 2.1

In Figure 2-13, considering the section from X' to Y, the following equations are valid:

$$\frac{X_1' - Z_1}{r_{11}} + \frac{X_2' - Z_1}{r_{12}} + \frac{Y_1 - Z_1}{r_{f1}} = 0$$

$$\frac{X_2' - Z_2}{r_{22}} + \frac{X_1' - Z_2}{r_{21}} + \frac{Y_2 - Z_2}{r_{f2}} = 0$$

In matrix form these equations become

$$\begin{pmatrix} \frac{1}{r_{11}} & \frac{1}{r_{12}} \\ \frac{1}{r_{21}} & \frac{1}{r_{22}} \end{pmatrix} \begin{pmatrix} X_1' \\ X_2' \end{pmatrix} + \begin{pmatrix} \frac{1}{r_{f1}} & 0 \\ 0 & \frac{1}{r_{f2}} \end{pmatrix} \begin{pmatrix} Y_1 \\ Y_2 \end{pmatrix}$$

$$- \begin{pmatrix} \frac{1}{r_{11}} + \frac{1}{r_{12}} + \frac{1}{r_{f1}} & 0 \\ 0 & \frac{1}{r_{22}} + \frac{1}{r_{21}} + \frac{1}{r_{f1}} \end{pmatrix} \begin{pmatrix} Z_1 \\ Z_2 \end{pmatrix} = 0 \qquad \ldots(2\text{-}18)$$

Equation (2-18) may be written in the form

$$FX' - QZ + CY = 0$$

or
$$C^{-1}FX' - C^{-1}QZ + Y = 0 \qquad \ldots(2\text{-}19)$$

Now since $Z_1 \approx 0$

and $Z_2 \approx 0$

we can set $Z = 0$

Therefore, $C^{-1}FX' = -Y$

Now from Figure 2-11 $AX' = Y$

therefore $$-A = C^{-1}F \qquad \ldots(2\text{-}20)$$

Also, from Figure 2-11,

$$AGX = (AG + I)Y \qquad \ldots(2\text{-}21)$$

Now from Figures 2-12 and 2-13 we can see that G is diagonal and that

$$G_{11} = G_{22} = G_c(s)$$

provided potentiometers 1 and 2 have identical settings. Therefore we can write equation (2-21) as

$$AX = (A + \frac{1}{G_c(s)} I)Y$$

The characteristic equation is

$$\left| A + \frac{1}{G_c(s)} I \right| = 0 \qquad \ldots(2\text{-}22)$$

Replacing $\frac{1}{G_c(s)}$ by $-\lambda$ yields the eigenvalue equation

$$\left| A - \lambda I \right| = 0 \qquad \ldots(2\text{-}23)$$

From equations (2-18) and (2-19) we have

$$F = \begin{pmatrix} \frac{1}{r_{11}} & \frac{1}{r_{12}} \\ \frac{1}{r_{21}} & \frac{1}{r_{22}} \end{pmatrix} \qquad C = \begin{pmatrix} \frac{1}{r_{f1}} & 0 \\ 0 & \frac{1}{r_{f2}} \end{pmatrix}$$

Substituting these values in equation (2-20) yields

$$A = \begin{pmatrix} \frac{r_{f1}}{r_{11}} & \frac{r_{f1}}{r_{12}} \\ \frac{r_{f2}}{r_{21}} & \frac{r_{f2}}{r_{22}} \end{pmatrix} \qquad \ldots(2\text{-}24)$$

The eigenvalue equation (2-23) becomes

$$\begin{pmatrix} \frac{r_{f1}}{r_{11}} - \lambda & \frac{r_{f1}}{r_{12}} \\ \frac{r_{f2}}{r_{21}} & \frac{r_{f2}}{r_{22}} - \lambda \end{pmatrix} = 0 \qquad \ldots(2\text{-}25)$$

Figure 2-13 shows that

$$r_{11} = r_{12} = r_{21} = r_{22} = r_{f1} = r_{f2} = 2M$$

Equation (2-25) becomes

$$\begin{vmatrix} 1 - \lambda & 1 \\ 1 & 1 - \lambda \end{vmatrix} = 0$$

Solving this determinant for the λ values yields

$$\lambda_1 = 0$$

$$\lambda_2 = 2$$

For the stability investigation we consider the Nyquist plot of

$$R_k(s) = \frac{1}{\lambda_k(s)} + G_c(s)$$

Figure 2-13 shows that

$$G_{11} = G_{22} = G_c(s) = \frac{k'}{1 + sT}$$

with T = 1, provided $\alpha_1 = \alpha_2$.

Figure 2-14 shows the Nyquist plot of this example.

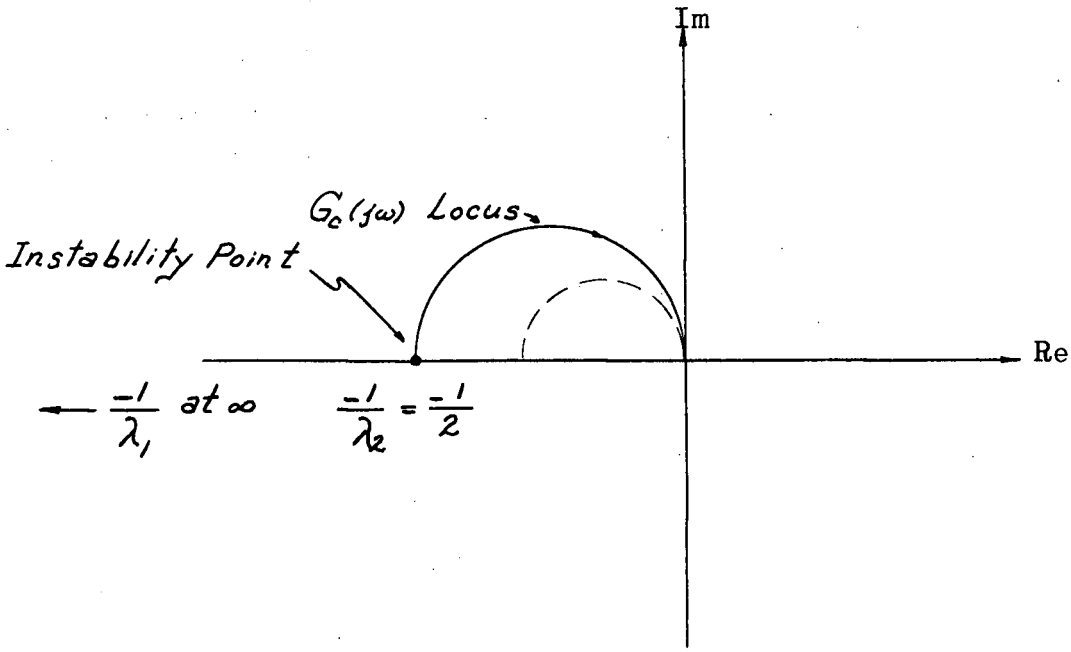

Figure 2-14. Nyquist Plot For Test Example 2-1

In the simulation tests, when $k' = 0.5$ the system became unstable. Thus experimental results verified the prediction that the system would be unstable if the gain k' of the $G_c(s)$ element reaches 0.5.

2.5 Test Example 2.2

As a second example, consider the system shown in Figures 2-15, 2-16 and 2-17.

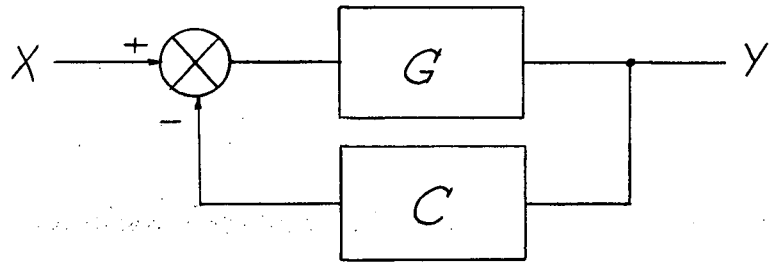

Figure 2-15. Matrix Form of Test Example 2.2

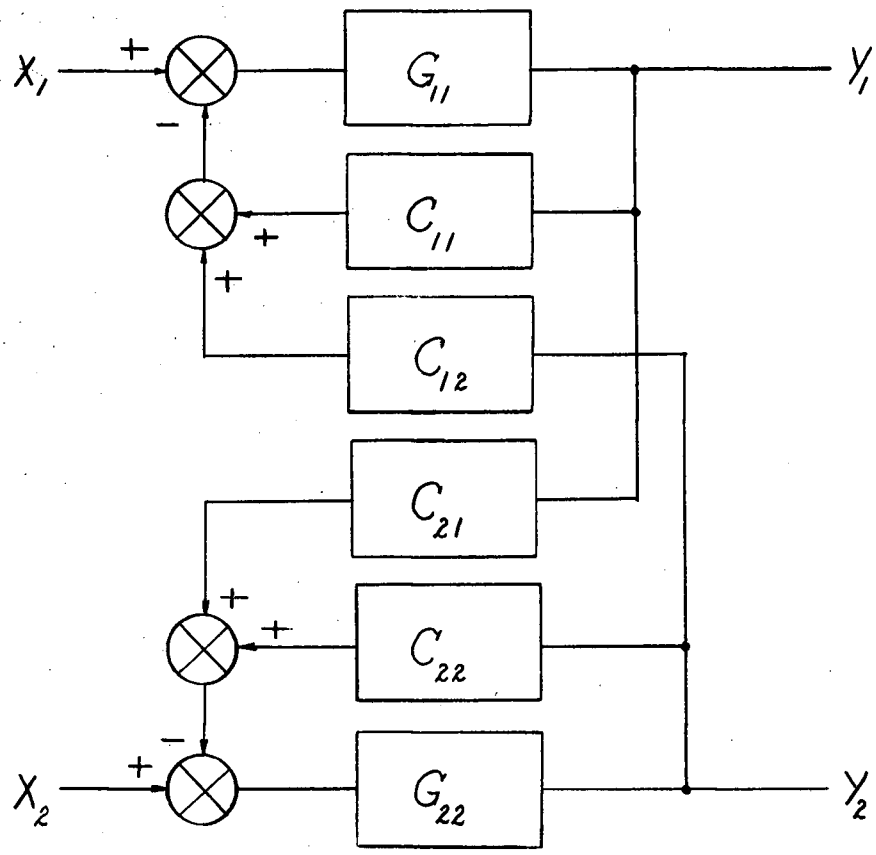

Figure 2-16. Circuit Form of Test Example 2.2

Analysis of the system of Figure 2-15 gives

$$GX = (GC + I)Y \qquad \ldots(2\text{-}26)$$

Analysis of the system of Figure 2-16 gives

$$\begin{pmatrix} G_{11} & 0 \\ 0 & G_{22} \end{pmatrix}\begin{pmatrix} X_1 \\ X_2 \end{pmatrix} = \begin{pmatrix} G_{11} & 0 \\ 0 & G_{22} \end{pmatrix}\begin{pmatrix} C_{11} & C_{12} \\ C_{21} & C_{22} \end{pmatrix} + \begin{pmatrix} 1 & 0 \\ 0 & 1 \end{pmatrix}\begin{pmatrix} Y_1 \\ Y_2 \end{pmatrix} \qquad \ldots(2\text{-}27)$$

By inspection it is apparent that equations (2-26) and (2-27) are identical.

Now suppose that

$$G_{11} = nG_c(s)$$

$$G_{22} = mG_c(s)$$

Then

$$G = G_c(s)\begin{pmatrix} n & 0 \\ 0 & m \end{pmatrix} = G_c(s)G'$$

Equation (2-26) becomes

$$G'X = \left(G'C + \frac{1}{G_c(s)}I\right)Y$$

The eigenvalue equation

$$\left|G'C - \lambda I\right| = 0 \qquad \ldots(2\text{-}28)$$

is obtained by replacing $\frac{1}{G_c(s)}$ with $-\lambda$. Equation (2-28) then takes the form

$$\begin{vmatrix} nC_{11} - \lambda & nC_{12} \\ mC_{21} & mC_{22} - \lambda \end{vmatrix} = 0 \qquad \ldots(2\text{-}29)$$

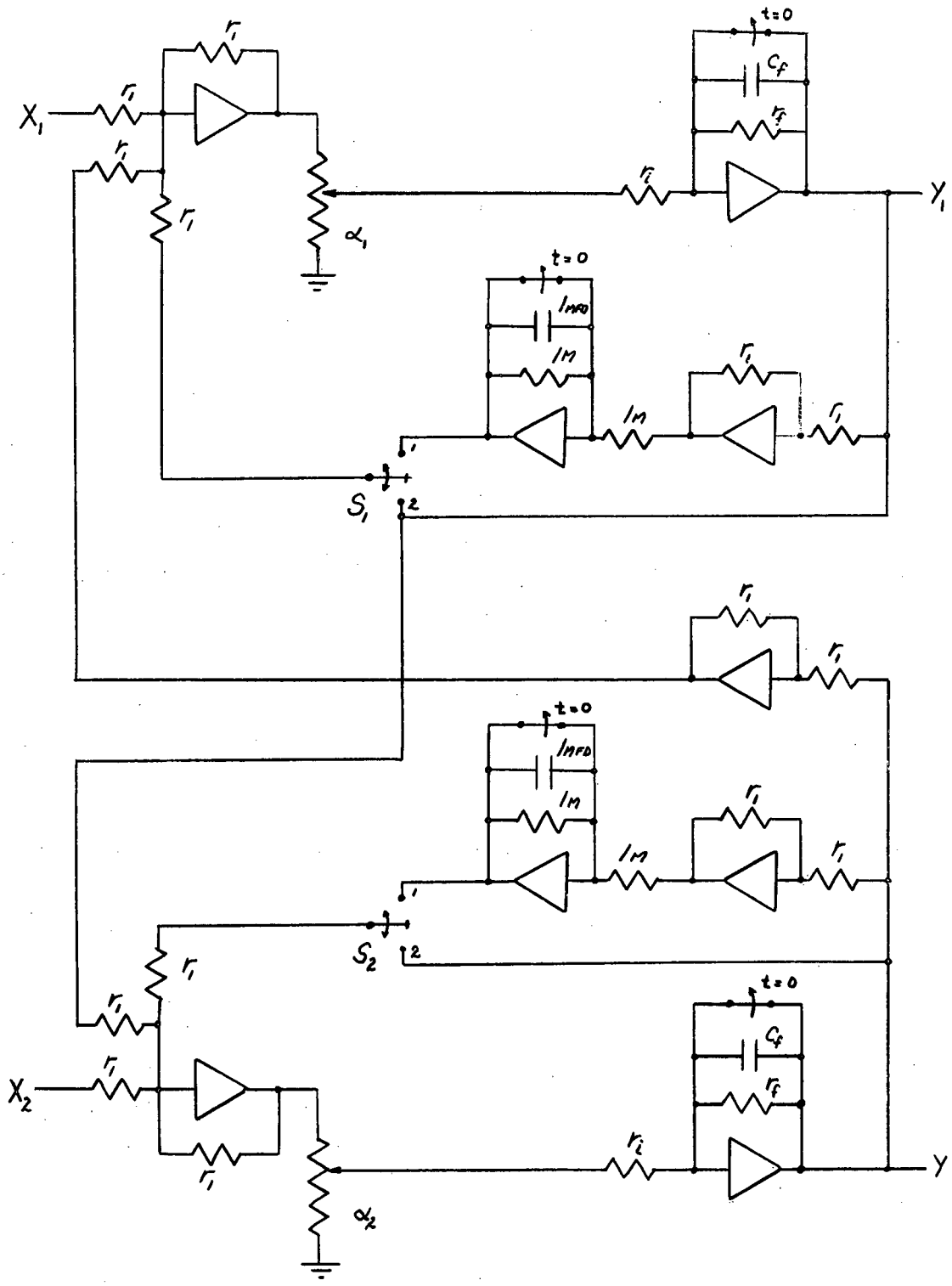

Figure 2-17. Computer Simulation Test Example 2.2

Figure 2-17 shows the analog computer simulation of the system where

$$G_c(s) = \frac{-\alpha\frac{r_f}{r_i}}{1 + sr_fc_f} = \frac{-K}{1 + sT}$$

With the switches s_1 and s_2 in position 2

$$C_{11} = C_{22} = 1$$

$$-C_{12} = C_{21} = 1$$

Now suppose we set $\alpha_1 = \alpha_2 = \alpha$

Therefore n = m and equation (2-29) becomes

$$\begin{vmatrix} 1 - \lambda & -1 \\ 1 & 1 - \lambda \end{vmatrix} = 0$$

which yields the eigenvalues

$$\lambda_1 = 1 + j$$

$$\lambda_2 = 1 - j$$

Now stability is determined by a Nyquist plot of

$$R_k(s) = \frac{1}{\lambda_k(s)} + G_c(s)$$

Now

$$\frac{-1}{\lambda_1} = \frac{-1}{1 + j}$$

and

$$\frac{-1}{\lambda_2} = \frac{-1}{1 - j}$$

Thus instability occurs when

$$\frac{-1}{\lambda_1} = \frac{-1}{1 + j} = \frac{-K}{1 + sT} = G_c(s)$$

which yields K = 1 and $\omega T = 1$

Component Values					Parameter Values Resulting in an Unstable System			
r_f	c_f	r_i	$T = r_f c_f$		α	$K = \alpha \frac{r_f}{r_i}$	freq.	ωT
10	.1	1.0	1		0.1	1	.158	1
5	1	1.0	5		0.2	1	.315	1

Table 2.1 Experimental Results of Test Example 2.1

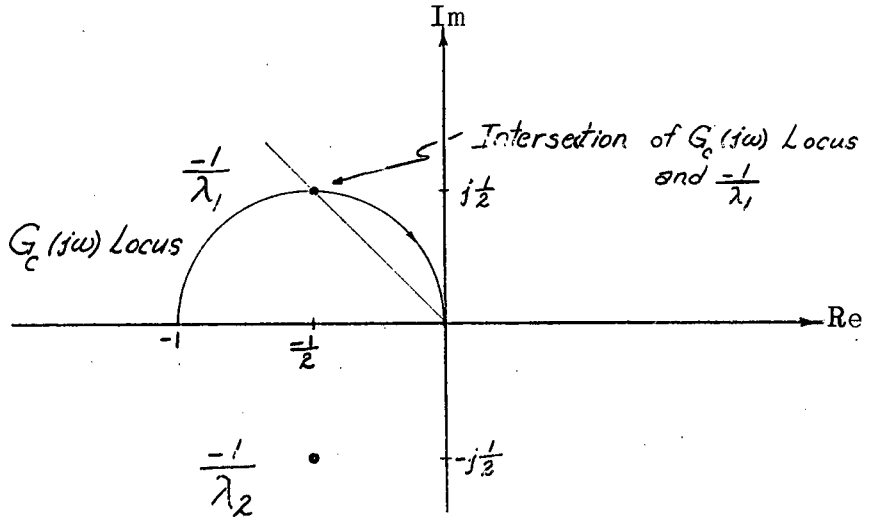

Figure 2-18. Nyquist Plot of Table 2.1

The experimental results agree with the predicted results.

Suppose now that n = 2 and m = 1. Equation (2-29) becomes

$$\begin{vmatrix} 2 - \lambda & -2 \\ 1 & 1 - \lambda \end{vmatrix} = 0$$

which yields the eigenvalues

$$\lambda_1 = 1.5 + j1.32$$

$$\lambda_2 = 1.5 - j1.32$$

Therefore,

$$\frac{-1}{\lambda_1} = \frac{-0.67}{1 + j0.88}$$

$$\frac{-1}{\lambda_2} = \frac{-0.67}{1 - j0.88}$$

Now instability occurs when

$$\frac{-1}{\lambda_1} = \frac{-0.67}{1 + j0.88} = \frac{-K}{1 + j\omega T}$$

which yields $K = 0.67$ and $\omega T = 0.88$

Component Values				Parameter Values Resulting in an Unstable System				
r_f	c_f	r_i	T	α_1	α_2	K	f	ωT
2	0.1	1	0.2	.68	.34	.68	.67	.86

Table 2.2 Experimental Results of Test Example 2.2

The experimental results verify the predicted results.

Thus we see that it is possible to determine a λ-value by choosing a G_c element and varying its parameters

until the system becomes unstable. As a somewhat more interesting case, suppose we determine a λ-locus by the same procedure.

Suppose switches S_1 and S_2 of Figure 2-17 are in position 1. This gives

$$C_{11} = C_{22} = \frac{1}{1 + s}$$

$$-C_{12} = C_{21} = 1$$

Now letting n = m, i.e., $\alpha_1 = \alpha_2$, the eigenvalue equation (2-29) becomes

$$\begin{vmatrix} \frac{1}{1 + s} - \lambda & -1 \\ 1 & \frac{1}{1 + s} - \lambda \end{vmatrix} = 0$$

which yields

$$\lambda_1(j\omega) = \frac{1}{1 + j\omega} + j$$

$$\lambda_2(j\omega) = \frac{1}{1 + j\omega} - j$$

As before, from equation (2-3), the system is unstable when $R_k(j\omega) = 0$. Figure 2-19 illustrates the Nyquist plot of $\frac{-1}{\lambda_k(j\omega)}$.

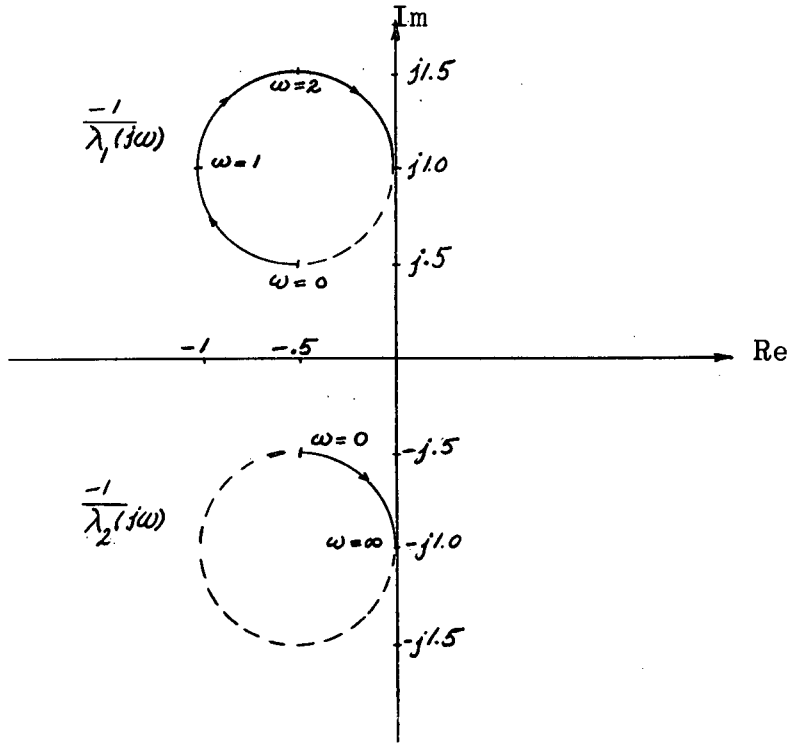

Figure 2-19. Nyquist Plot of $\frac{-1}{\lambda_k(j\omega)}$

In this particular case it is easier to plot $\lambda_k(j\omega)$ and $\frac{-1}{G_c(j\omega)}$ rather than $\frac{-1}{\lambda_k(j\omega)}$ and $G_c(j\omega)$. This is shown in Figure 2-20.

If the $\frac{-1}{G_c(j\omega)}$ locus intersects the critical λ-locus, at a critical frequency ω_c, the system is unstable. Thus, it has been shown possible to determine the λ-locus experimentally by choosing a convenient G_c. The transfer function G_c can be suitably varied by selecting various T's, i.e., r_f and c_f, and adjusting its gain, i.e., α_1 and α_2, until the system is on the verge of instability and then measuring the frequency of free oscillation of the system.

Now $$\frac{-1}{G_c(j\omega)} = \frac{1 + j\omega T}{K}$$

Figure 2-20 shows that for each value of T selected, two points of the critical locus may be determined. They are

$$\frac{-1}{G_c} = \frac{1}{K'} + \frac{j\omega' T}{K'}$$

and $$\frac{-1}{G_c} = \frac{1}{K''} + \frac{j\omega'' T}{K''}$$

where

$$\frac{\omega'' T}{K''} = \frac{\omega' T}{K'} \quad \text{but } K'' \neq K'$$

The experimental results given in Table 2.3 and Figures 2-21, 2-22, and 2-23 verify the predicted results.

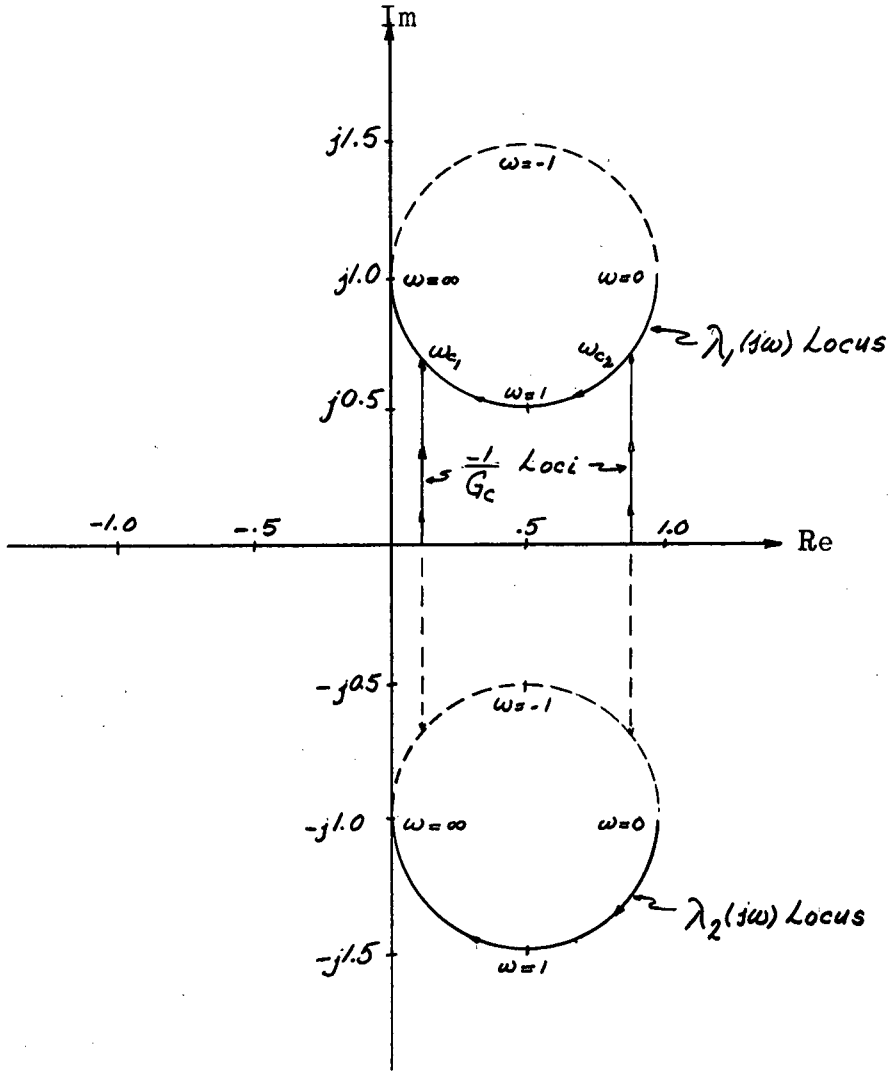

Figure 2-20. Nyquist Plot of $\lambda_k(j\omega)$ and $\frac{-1}{G_c(j\omega)}$

r_i	r_f	c_f	T	K'	ω'	$\frac{1}{K'}$	$\frac{\omega' T}{K'}$	K''	ω''	$\frac{1}{K''}$	$\frac{\omega'' T}{K''}$	
1.0	10.0	0.105	1.05	1.70	0.805	0.588	0.497	2.58	1.22	0.388	0.497	
↓	↓	0.11	1.10	1.58	0.73	0.633	0.506	2.90	1.34	0.345	0.508	
		0.12	1.20	1.45	0.642	0.69	0.531	3.50	1.53	0.286	0.524	
		0.13	1.30	1.37	0.582	0.73	0.553	4.03	1.70	0.248	0.548	
		0.14	1.40	1.32	0.535	0.757	0.567	4.60	1.85	0.218	0.565	Fig. 2-21
		0.15	1.50	1.27	0.495	0.787	0.585	5.13	1.93	0.195	0.565	
		0.175	1.75	1.20	0.433	0.83	0.632	6.55	2.27	0.153	0.607	
		0.20	2.0	1.15	0.376	0.87	0.652	8.00	2.53	0.125	0.632	
0.5		0.30	3.0	1.08	0.267	0.927	0.742	15.50	3.56	0.065	0.69	
↓		0.06	0.60	1.43	1.25	0.70	0.525	3.54	3.05	0.283	0.517	
		0.07	0.70	1.31	1.06	0.763	0.567	4.62	3.60	0.217	0.546	
		0.08	0.80	1.24	0.906	0.805	0.585	5.69	4.03	0.176	0.568	Fig. 2-22
		0.09	0.90	1.20	0.83	0.834	0.622	6.85	4.65	0.146	0.612	
		0.10	1.0	1.16	0.75	0.862	0.650	8.00	5.02	0.125	0.628	
		0.15	1.50	1.09	0.53	0.918	0.732	15.52	12.6	0.065	0.705	
		0.01	0.10	0.705	0.647	1.42	0.092	1.73	1.54	0.578	0.089	
		0.02	0.20	0.640	0.532	1.56	0.166	2.29	1.86	0.437	0.162	
		0.03	0.30	0.605	0.465	1.65	0.231	2.85	2.09	0.350	0.220	
		0.04	0.40	0.580	0.412	1.72	0.248	3.46	2.36	0.289	0.273	
		0.05	0.50	0.565	0.383	1.77	0.338	4.07	2.60	0.246	0.320	
		0.06	0.60	0.555	0.341	1.81	0.368	4.74	2.78	0.211	0.352	Fig. 2-23
		0.07	0.70	0.545	0.322	1.84	0.416	5.44	2.88	0.184	0.370	
		0.08	0.80	0.540	0.298	1.85	0.441	6.16	3.24	0.162	0.420	
		0.09	0.90	0.538	0.279	1.86	0.468	6.93	3.34	0.144	0.434	
		0.10	1.0	0.530	0.265	1.89	0.50	7.70	3.65	0.130	0.473	
		0.15	1.50	0.523	0.205	1.91	0.59	12.66	4.63	0.079	0.550	

Table 2.3 Experimental Results for Test Example 2.2

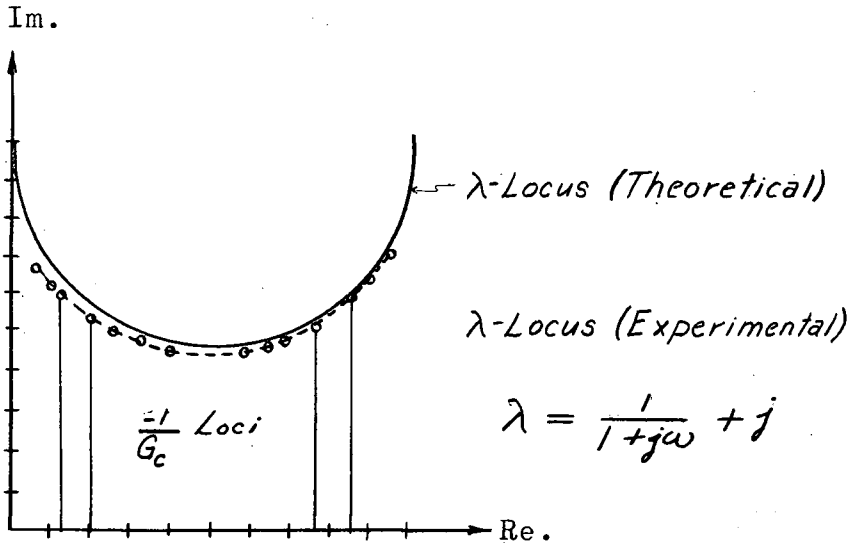

Figure 2-21 λ-Locus from Table 2.3

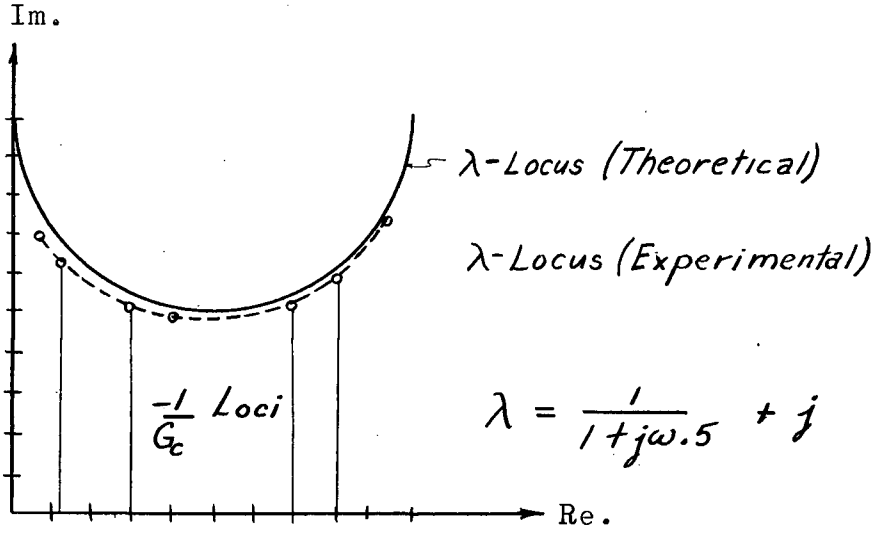

Figure 2-22 λ-Locus from Table 2.3

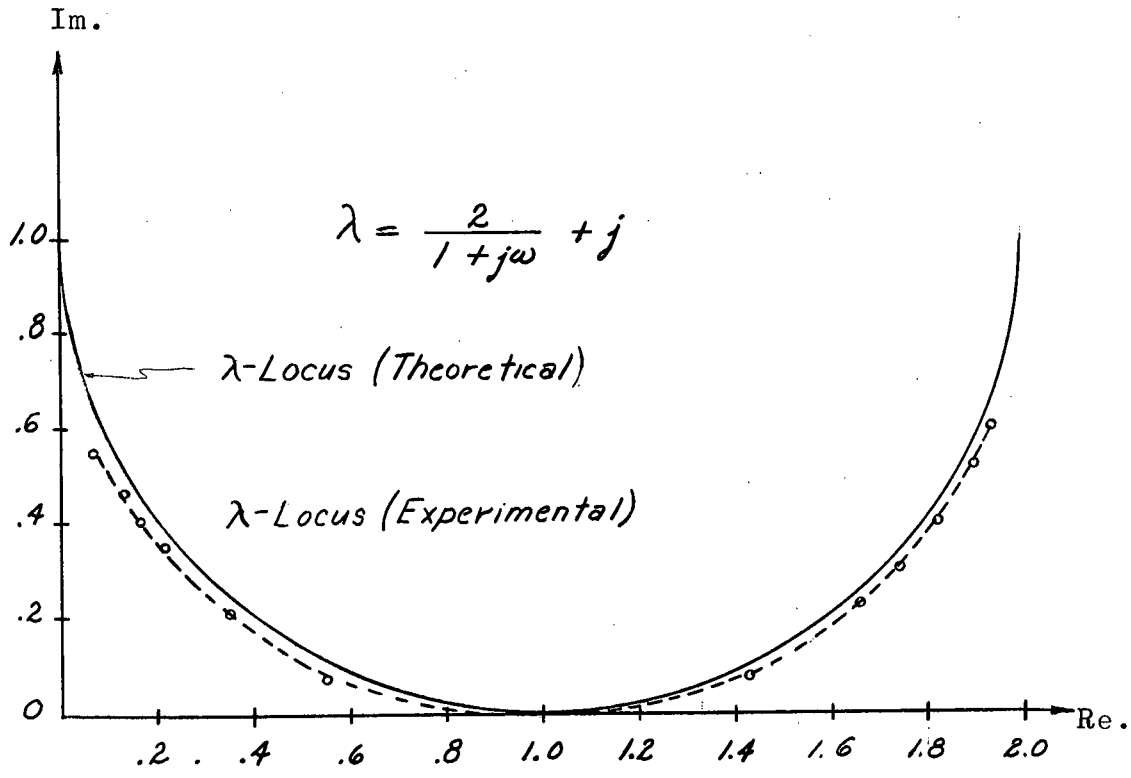

Figure 2-23 λ-Locus from Table 2.3

In general, for a complex system, the calculation of the critical λ-loci is very complicated even with the aid of digital computers. Using a convenient variable element, $G_c(s)$, in a simulated system, it is possible to find the critical λ-locus relatively easily. The variable element is adjusted until the system is on the verge of instability. This determines a point on the critical λ-locus. After the critical λ-locus is completely determined it can be used to design a suitable variable element for the closed-loop system.

3. NONINTERACTION

In the analysis of multivariable feedback control systems much effort has been spent developing methods for attaining noninteraction, that is for attaining a system whose input variable, say X_k, controls only its corresponding output variable Y_k. Stated mathematically, the condition for noninteraction is that the closed-loop transfer matrix H is diagonal. Once noninteraction has been accomplished, the system can be treated as consisting of n single-variable systems.

Boksenbom and Hood[10] did some of the earliest work on achieving noninteraction in multivariable systems. Their major interest was in obtaining the conditions for noninteraction in linear multivariable systems with particular emphasis on an engine-type problem. Meerov[11] discussed a special class of systems which became noninteracting if the gains of the system are increased without limit. In general this means increasing loop gains until the effect of the cross-coupling elements become negligible.

Another method of achieving noninteraction consists of a trial and error selection of elementary transformations which result in the diagonalization of the open-loop matrix. There is no unique method of diagonalizing the open-loop transfer matrix. A convenient method, which usually results

in simple physically realizable elements, will now be discussed.

3.1 Diagonalization of Open-Loop Transfer Matrix

To illustrate this method, consider Figure 3-1

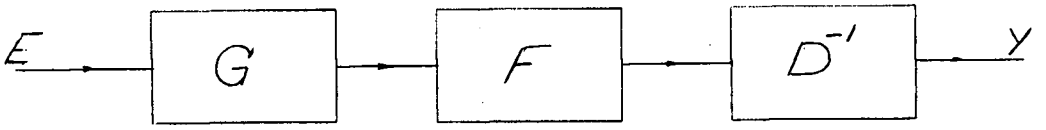

Figure 3-1 Open-Loop System

where E and Y are column matrices where elements are the input and output signals respectively and G, F and D^{-1} are n x n transfer matrices. G is taken to be diagonal and is called the amplification or gain matrix, F is the forcing matrix and D^{-1} is called the dynamical matrix. Analysis of Figure 3-1 yields

$$D^{-1}FGE = Y \qquad \ldots(3\text{-}1)$$

or, premultiplying both sides by D,

$$FGE = DY \qquad \ldots(3\text{-}2)$$

One method of diagonalizing a 2 x 2 system is shown in Figure 3-2 where

$$X = \begin{pmatrix} X_1 \\ X_2 \end{pmatrix} \qquad Y = \begin{pmatrix} Y_1 \\ Y_2 \end{pmatrix}$$

$$E = \begin{pmatrix} X_1 - Y_1 \\ X_2 - Y_2 \end{pmatrix} \qquad G = \begin{pmatrix} G_{11} & 0 \\ 0 & G_{22} \end{pmatrix}$$

$$F = \begin{pmatrix} F_{11} & 0 \\ 0 & F_{22} \end{pmatrix} \qquad D = \begin{pmatrix} D_{11} & D_{12} \\ D_{21} & D_{22} \end{pmatrix}$$

and T_2, C_2 and C_1 represent transformation and compensation matrices which are to be determined. Analysis of Figure 3-2 yields

$$D^{-1}FGC_1C_2T_2E = Y \qquad \ldots(3\text{-}3)$$

or

$$D^{-1}FGC_1C_2T_2(X - Y) = Y \qquad \ldots(3\text{-}4)$$

According to the design philosophy to be discussed, the open-loop transfer matrix $D^{-1}FGC_1C_2T_2$ is to be diagonalized and the diagonal elements are to be suitably chosen to realize good dynamic performance. For the particular configuration shown in Figure 3-2, this method results in a diagonal H (closed-loop transfer matrix). Suppose we write the D matrix in the factored form

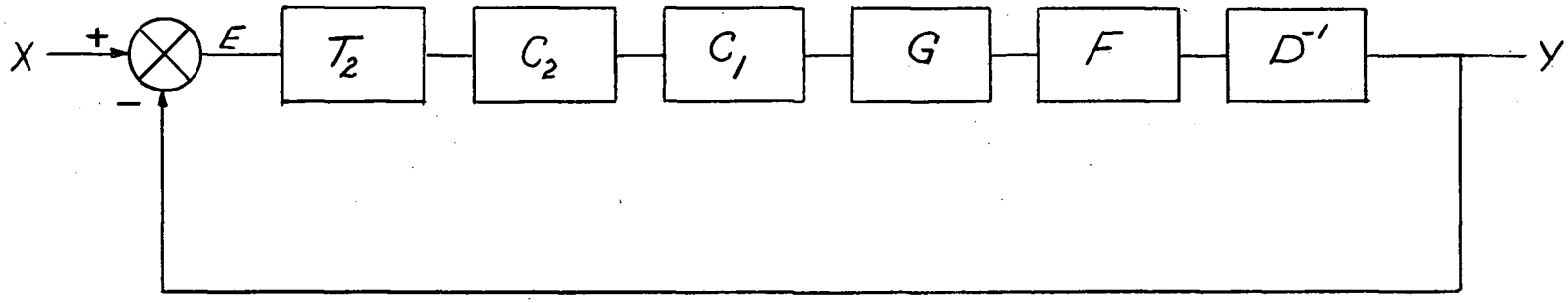

Figure 3-2 Diagonalization of Open-Loop Transfer Matrix

$$D = T_1 D' T_2 \qquad \ldots(3\text{-}5)$$

The inverse dynamical matrix is

$$D^{-1} = T_2^{-1}(D')^{-1}T_1^{-1} \qquad \ldots(3\text{-}6)$$

Now choose T_1 so that

$$T_2 D^{-1} F G C_1 = (D')^{-1} T_1^{-1} F G C_1 \qquad \ldots(3\text{-}7)$$

$$= (D')^{-1} G \qquad \ldots(3\text{-}8)$$

This requires that

$$T_1 G = F G C_1 \qquad \ldots(3\text{-}9)$$

Thus

$$T_2^{-1}(D')^{-1} G C_2 T_2 X = (T_2^{-1}(D')^{-1} G C_2 T_2 + I)Y \qquad \ldots(3\text{-}10)$$

The matrices T_1, T_2, C_1, C_2 and D' will now be determined. Equation (3-9) is satisfied if a new matrix C_1' is defined by the matrix commutation

$$G C_1 = C_1' G \qquad \ldots(3\text{-}11)$$

and C_1' is chosen to be

$$C_1' = F^{-1} T_1 \qquad \ldots(3\text{-}12)$$

Matrix T_1 is chosen to have the form

$$T_1 = F_c \begin{pmatrix} 1 & T'_{12} \\ T'_{21} & 1 \end{pmatrix} \qquad \ldots(3\text{-}13)$$

where F_c is a suitable common factor and T'_{12} and T'_{21} are transfer functions which are to be determined. Postmultiplication of equation (3-5) with T_2^{-1} yields

$$DT_2^{-1} = T_1 D' \qquad \ldots(3\text{-}14)$$

The design philosophy is to diagonalize the open-loop transfer matrix and suitably choose the diagonal elements to realize both good dynamic performance and simple, physically realizable, compensating elements. This objective can be achieved if D' has the form

$$D' = \frac{1}{F_c} \begin{pmatrix} D'_{11} & 0 \\ 0 & D'_{22} \end{pmatrix} \qquad \ldots(3\text{-}15)$$

and if

$$T_2^{-1} = \begin{pmatrix} 1 & \alpha_{12} \\ \alpha_{21} & 1 \end{pmatrix} \qquad \ldots(3\text{-}16)$$

where α_{12} and α_{21} are constants. The inverse matrix is

$$T_2 = \frac{1}{1 - \alpha_{12}\alpha_{21}} \begin{pmatrix} 1 & -\alpha_{12} \\ -\alpha_{21} & 1 \end{pmatrix} \qquad \ldots(3\text{-}17)$$

where $1 - \alpha_{12}\alpha_{21} \neq 0$

Substituting equations (3-13), (3-15) and (3-16) into equation (3-14) gives

$$\begin{pmatrix} D_{11} & D_{12} \\ D_{21} & D_{22} \end{pmatrix} \begin{pmatrix} 1 & \alpha_{12} \\ \alpha_{21} & 1 \end{pmatrix} = F_c \begin{pmatrix} 1 & T'_{12} \\ T'_{21} & 1 \end{pmatrix} \frac{1}{F_c} \begin{pmatrix} D'_{11} & 0 \\ 0 & D'_{22} \end{pmatrix}$$

or

$$\begin{pmatrix} D_{11} + D_{12}\alpha_{21} & D_{11}\alpha_{12} + D_{12} \\ D_{21} + D_{22}\alpha_{21} & D_{21}\alpha_{12} + D_{22} \end{pmatrix} = \begin{pmatrix} D'_{11} & D'_{22}T'_{12} \\ D'_{11}T'_{21} & D'_{22} \end{pmatrix} \quad \ldots(3\text{-}18)$$

Equating elements yields

$$D'_{11} = D_{11} + D_{12}\alpha_{21} \quad \ldots(3\text{-}19)$$

$$D'_{22} = D_{22} + D_{21}\alpha_{12} \quad \ldots(3\text{-}20)$$

$$T'_{12} = \frac{D_{11}\alpha_{12} + D_{12}}{D'_{22}} \quad \ldots(3\text{-}21)$$

$$T'_{21} = \frac{D_{22}\alpha_{21} + D_{21}}{D'_{11}} \quad \ldots(3\text{-}22)$$

Combining equations (3-19), (3-20), (3-21) and (3-22) gives

$$T'_{12} = \frac{D_{12} + \alpha_{12}D_{11}}{D_{22} + \alpha_{12}D_{21}} \quad \ldots(3\text{-}23)$$

$$T_{21}' = \frac{D_{21} + \alpha_{21} D_{22}}{D_{11} + \alpha_{21} D_{12}} \qquad \ldots(3\text{-}24)$$

Thus T_1 has now been determined in terms of the D matrix and the two constants α_{12} and α_{21}. T_2 is given by equation (3-17). C_1' and, hence, C_1 can be determined from T_1 (see equation (3-12)). C_2 is selected to be a diagonal compensating matrix. Therefore, all elements of the diagonalized system have been determined.

There is a restriction on α_{12} and α_{21} in that the transfer functions given by equations (3-23) and (3-24) must be physically realizable. It is evidently desirable to have simple physically realizable elements for T_1 and T_2 which allow high loop gains and yield a stable system. Once suitable transformations are found, more quantitative root-locus methods may be applied to determine gain parameters, etc., for the variable elements. The suitability of the design may then be tested by simulation studies.

3.2 Illustrative Example

As an example, let us apply this procedure to the system shown in Figure 3-3. Analysis of this system yields

$$\begin{pmatrix} F_{11} & 0 \\ 0 & F_{22} \end{pmatrix} \begin{pmatrix} G_{11} & 0 \\ 0 & G_{22} \end{pmatrix} \begin{pmatrix} E_1 \\ E_2 \end{pmatrix} = \begin{pmatrix} 1 & F_{11}J_{11} \\ F_{22}J_{22} & 1 \end{pmatrix} \begin{pmatrix} Y_1 \\ Y_2 \end{pmatrix} \qquad \ldots(3\text{-}25)$$

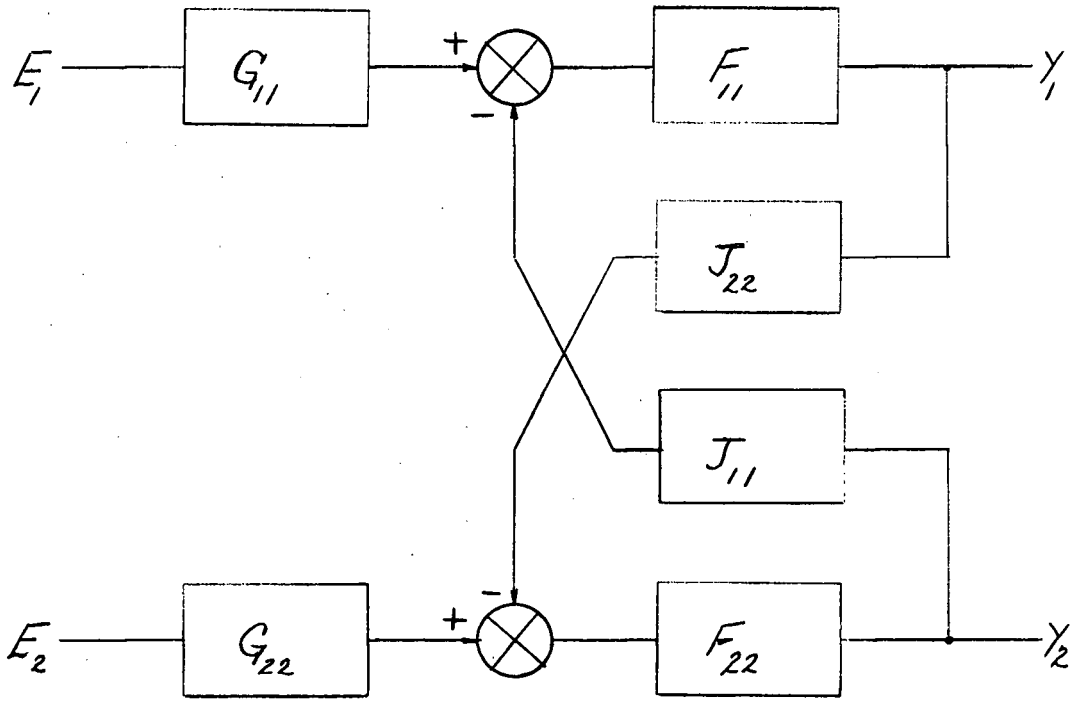

Figure 3-3 Two-Axis Tracking System

A comparison of equations (3-25) and (3-2) shows that

$$G = \begin{pmatrix} G_{11} & 0 \\ 0 & G_{22} \end{pmatrix} \qquad F = \begin{pmatrix} F_{11} & 0 \\ 0 & F_{22} \end{pmatrix} \qquad \ldots(3\text{-}26)$$

$$D = \begin{pmatrix} 1 & F_{11}J_{11} \\ F_{22}J_{22} & 1 \end{pmatrix}$$

If C_2 is assumed diagonal, we have

$$C_2 = \begin{pmatrix} C_{2_{11}} & 0 \\ 0 & C_{2_{22}} \end{pmatrix} \qquad \ldots(3\text{-}27)$$

Equation (3-17) gives

$$T_2 = \frac{1}{1 - \alpha_{12}\alpha_{21}} \begin{pmatrix} 1 & -\alpha_{12} \\ -\alpha_{21} & 1 \end{pmatrix} \qquad \ldots(3\text{-}19)$$

If G is diagonal and $G_{11} = G_{22}$, it follows from the matrix commutation

$$GC_1 = C_1'G \qquad \ldots(3\text{-}13)$$

and equation (3-12) that

$$C_1 = C_1' = \frac{1}{F_{11}F_{22}} \begin{pmatrix} F_{22} & 0 \\ 0 & F_{11} \end{pmatrix} T_1 = \begin{pmatrix} \frac{1}{F_{11}} & 0 \\ 0 & \frac{1}{F_{22}} \end{pmatrix} T_1 \qquad \ldots(3\text{-}28)$$

Equation (3-13) gives

$$T_1 = F_c \begin{pmatrix} 1 & T_{12}' \\ T_{21}' & 1 \end{pmatrix} \qquad \ldots(3\text{-}15)$$

Therefore

$$C_1 = \begin{pmatrix} \frac{1}{F_{11}} & 0 \\ 0 & \frac{1}{F_{22}} \end{pmatrix} F_c \begin{pmatrix} 1 & T_{12}' \\ T_{21}' & 1 \end{pmatrix} \qquad \ldots(3\text{-}29)$$

Now if $F_{11} = F_{22} = F_c$, we obtain

$$C_1 = \begin{pmatrix} 1 & T'_{12} \\ T'_{21} & 1 \end{pmatrix} \qquad \ldots(3\text{-}30)$$

Substituting the values of the D matrix elements into equations (3-23) and (3-24) gives

$$T'_{12} = \frac{\alpha_{12} + J_{11}F_{11}}{1 + \alpha_{12}J_{22}F_{22}} \qquad \ldots(3\text{-}31)$$

$$T'_{21} = \frac{\alpha_{21} + J_{22}F_{22}}{1 + \alpha_{21}J_{11}F_{11}} \qquad \ldots(3\text{-}32)$$

From equation (3-3) the open-loop transfer matrix B is

$$B = D^{-1}FGC_1C_2T_2 \qquad \ldots(3\text{-}33)$$

The design philosophy is to diagonalize B and suitably choose elements B_{11} and B_{22}. Let us consider the case where

$$\begin{aligned} -J_{11} &= J_{22} = J(s) \\ F_{11} &= F_{22} = F(s) \\ G_{11} &= G_{22} = G(s) \\ C_{2_{11}} &= C_{2_{22}} = C_2(s) \end{aligned} \qquad \ldots(3\text{-}34)$$

Substituting these values into the matrix B and cancelling

where possible we obtain

$$B = \frac{C_2FG}{(1 + (JF)^2)(1 - \alpha_{12}\alpha_{21})}$$

$$\begin{pmatrix} 1 + JFT'_{21} - \alpha_{21}(T'_{12} + JF) & T'_{12} + JF - \alpha_{12}(1 + JFT'_{21}) \\ T'_{21} - JF - \alpha_{21}(1 - JFT'_{12}) & 1 - JFT'_{12} - \alpha_{12}(T'_{21} - JF) \end{pmatrix}$$

$$B = \frac{C_2FG}{(1 + (JF)^2)(1 - \alpha_{12}\alpha_{21})} \begin{pmatrix} B'_{11} & B'_{12} \\ B'_{21} & B'_{22} \end{pmatrix} \qquad \ldots(3\text{-}35)$$

where we have set $J = J(s)$, $F = F(s)$, etc., to simplify the notation. Now for noninteraction we set

$$B'_{12} = -\alpha_{12} - \alpha_{12}JFT'_{21} + T'_{12} + JF = 0 \qquad \ldots(3\text{-}36)$$

$$B'_{21} = -\alpha_{21} + \alpha_{21}JFT'_{12} + T'_{21} - JF = 0 \qquad \ldots(3\text{-}37)$$

These two equations are satisfied if we set

$$\alpha_{12} = -\alpha_{21} = \alpha \qquad \ldots(3\text{-}38)$$

$$T'_{12} = -T'_{21} = T' \qquad \ldots(3\text{-}39)$$

These relationships and equations (3-31) and (3-32) yield

$$T' = \frac{\alpha - JF}{1 + \alpha JF} \qquad \ldots(3\text{-}40)$$

Solving equation (3-35) for B_{11} and B_{22} using equations (3-38), (3-39) and (3-40) yields

$$B_{11} = B_{22} = \frac{C_2FG}{1 + \alpha JF}$$

The final open-loop transfer matrix is

$$B = \begin{pmatrix} \frac{C_2FG}{1 + \alpha JF} & 0 \\ 0 & \frac{C_2FG}{1 + \alpha JF} \end{pmatrix}$$

Thus by means of this choice of T_1 and T_2 the open-loop transfer matrix is diagonalized and the system design reduces to a discussion of the two noninteracting systems each having an open-loop transfer function of the form

$$B_{kk} = \frac{C_2'FG}{1 + \alpha JF}$$

The choice of compensating networks and gain constants for these systems can be found by conventional graphical methods.

This procedure does not necessarily lead to the optimum design because it requires the open-loop transfer matrix to be diagonalized. This may not always be desirable since the off-diagonal elements often improve system performance. The method does, however, allow the designer

to investigate the possibilities with relatively few constraints on the selection of the compensating elements and avoids the practical difficulties of a purely theoretical approach.

4. THE TWO-AXIS TRACKING SYSTEM A COMPARATIVE STUDY OF THE EIGENVALUE METHOD AND THE DIAGONALIZATION METHOD

This chapter deals with a treatment of the two-axis tracking system shown in Figure 4-1. This particular configuration has been discussed by a number of authors. Krasovskii[6] has dealt with it as an antisymmetric system, i.e., the cross-coupling transfer functions are the negative of each other

$$J_{11} = -J_{22}$$

Krasovskii defines the input and output signals as complex

$$X = X_1 + jX_2 \qquad Y = Y_1 + jY_2$$

This procedure enables him to reduce the system to an equivalent single variable system which he then treats in the conventional Nyquist manner. Newman's[7] paper deals with the analysis of a similiar system. The methods of both these authors are restricted to two variable systems with the necessary symmetry.

4.1 Open-Loop Two-Axis Tracking System

Consider now the two-axis tracking system shown in block diagram form in Figure 4-1. Analysis of the open-loop system ($C_{11} = C_{22} = 0$) yields

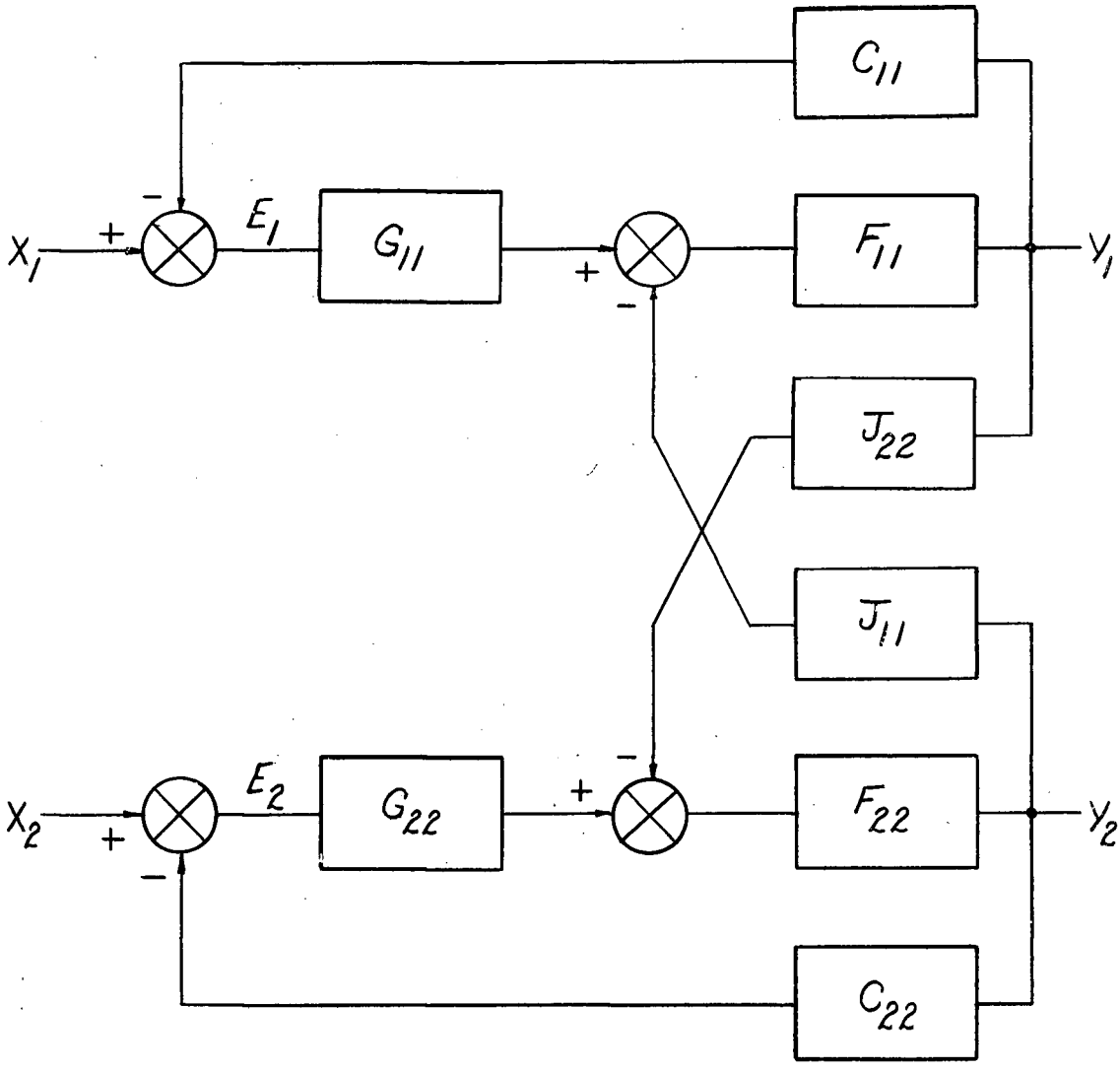

Figure 4-1 Two-Axis Tracking System

$$F_{11}G_{11}E_1 - F_{11}J_{11}Y_2 = Y_1 \qquad \ldots(4\text{-}1)$$

$$F_{22}G_{22}E_2 - F_{22}J_{22}Y_1 = Y_2 \qquad \ldots(4\text{-}2)$$

In matrix form these equations become

$$\begin{pmatrix} F_{11} & 0 \\ 0 & F_{22} \end{pmatrix}\begin{pmatrix} G_{11} & 0 \\ 0 & G_{22} \end{pmatrix}\begin{pmatrix} E_1 \\ E_2 \end{pmatrix} = \begin{pmatrix} 1 & F_{11}J_{11} \\ F_{22}J_{22} & 1 \end{pmatrix}\begin{pmatrix} Y_1 \\ Y_2 \end{pmatrix} \qquad \ldots(4\text{-}3)$$

From equation (4-3) the characteristic equation

$$\begin{vmatrix} 1 & F_{11}J_{11} \\ F_{22}J_{22} & 1 \end{vmatrix} = 0 \qquad \ldots(4\text{-}4)$$

is obtained. Consider now the case where $F_{11} = F_{22} = F$. If the stability of open-loop is to be investigated, the eigenvalue method can be used. F is then replaced by λ. Substituting into equation (4-4) and solving for the eigenvalues yields

$$\lambda_{1,2} = \frac{\pm 1}{\sqrt{J_{11}J_{22}}} \qquad \ldots(4\text{-}5)$$

The eigenvalue equation has thus been factored in the form

$$(\lambda - \lambda_1)(\lambda - \lambda_2) = 0$$

or

$$(F - \lambda_1)(F - \lambda_2) = 0 \qquad \ldots(4\text{-}6)$$

Stability is then determined by a Nyquist plot of the function (see Figure 4-2).

$$R_k(s) = -\lambda_k(s) + F(s) \qquad \ldots(4\text{-}7)$$

$R_k(j\omega)$ may be called a stability vector. The system will oscillate at the frequency ω_c if

$$R_k(j\omega_c) = 0$$

4.2 Closed-Loop Two Axis Tracking System

Let us now consider the closed-loop system of Figure 4-1. Analysis yields the following matrix equation

$$\begin{vmatrix} F_{11}G_{11} & 0 \\ 0 & F_{22}G_{22} \end{vmatrix} \begin{vmatrix} X_1 \\ X_2 \end{vmatrix} = \begin{vmatrix} 1 + C_{11}G_{11}F_{11} & J_{11}F_{11} \\ J_{22}F_{22} & 1 + C_{22}G_{22}F_{22} \end{vmatrix} \begin{vmatrix} Y_1 \\ Y_2 \end{vmatrix} \qquad \ldots(4\text{-}8)$$

Now suppose we let

$$J_{11} = J_{22} = J \qquad F_{11} = F_{22} = F$$

$$G_{11} = G_{22} = G \qquad C_{11} = C_{22} = C$$

Equation (4-8) yields the characteristic equation

$$\begin{vmatrix} 1 + CGF & JF \\ JF & 1 + CGF \end{vmatrix} = 0 \qquad \ldots(4\text{-}9)$$

The eigenvalue equation is obtained if J is replaced by λ. This equation then gives the eigenvalues

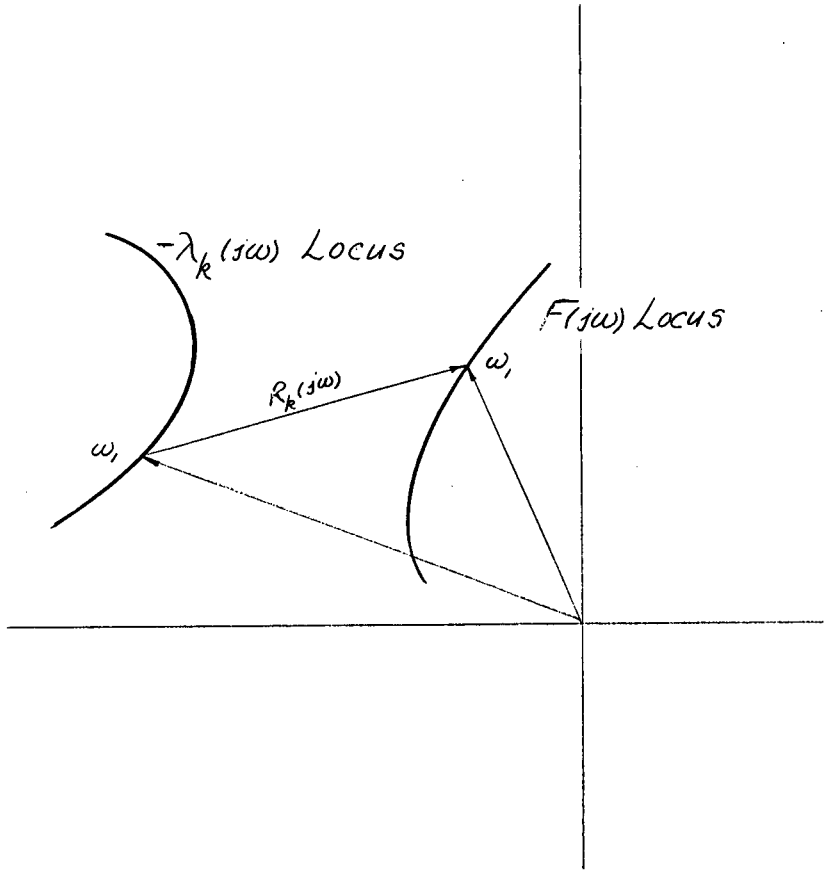

Figure 4-2 Nyquist Plot of $R_k(j\omega) = -\lambda_k(j\omega) + F(j\omega)$

$$\lambda_{1,2} = \pm \frac{1}{F} + CG \qquad \ldots(4\text{-}10)$$

In the case where $J_{11} = -J_{22} = J$, the eigenvalues are

$$\lambda_{1,2} = \pm j \frac{1}{F} + CG \qquad \ldots(4\text{-}11)$$

4.3 Simulation Study of Two-Axis Tracking Systems

In the two-axis tracking system shown in Figure 4-3, we have the following transfer functions:

$G_{11} = G_{22} = K_G$	Power Amplifier Gain
$F_{11} = F_{22} = \dfrac{K_F}{s(1 + sT_a)(1 + sT_b)}$	Transfer Function of an Amplifier
$J_{11} = J_{22} = as$	Transfer Function due to Gyroscopic Torque

Practical difficulties arise if one attempts to simulate the derivative elements as. The configuration shown in Figure 4-4, which has the same response as that of Figure 4-3, includes no derivative elements and was used for analog computer simulation. To realize the transfer function F' (see Figure 4-4) with one operational amplifier the network discussed in Appendix I was used. The network analog of the system is shown in Figure 4-5. From Appendix I we have

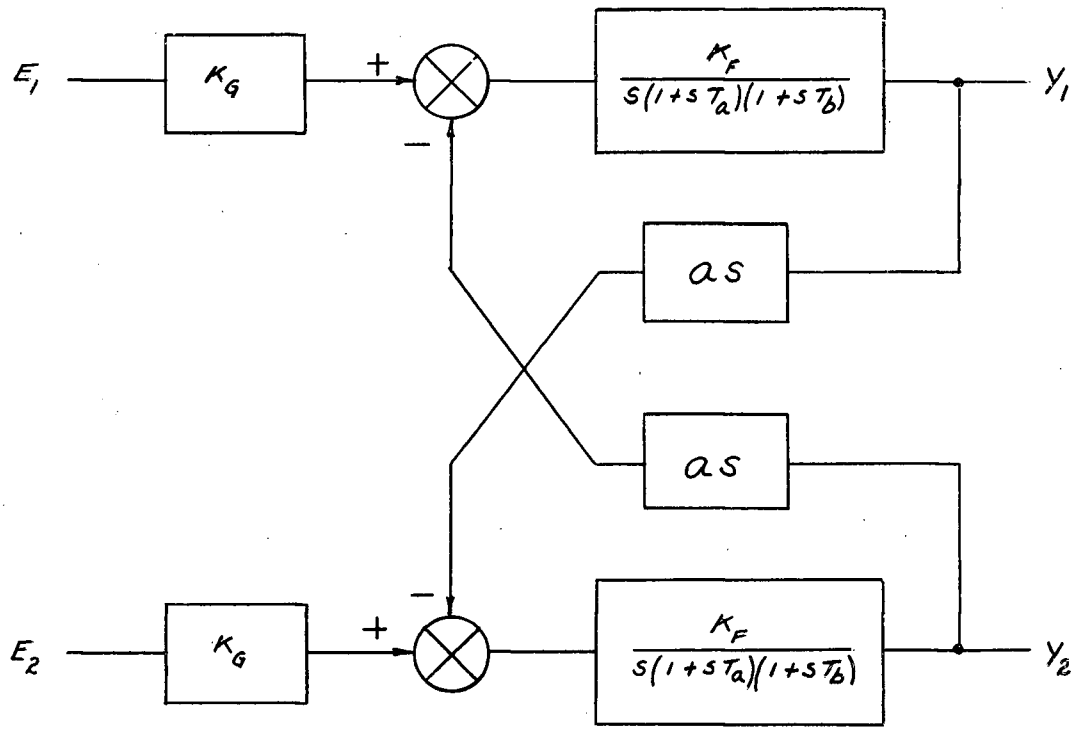

Figure 4-3 Two-Axis Tracking System

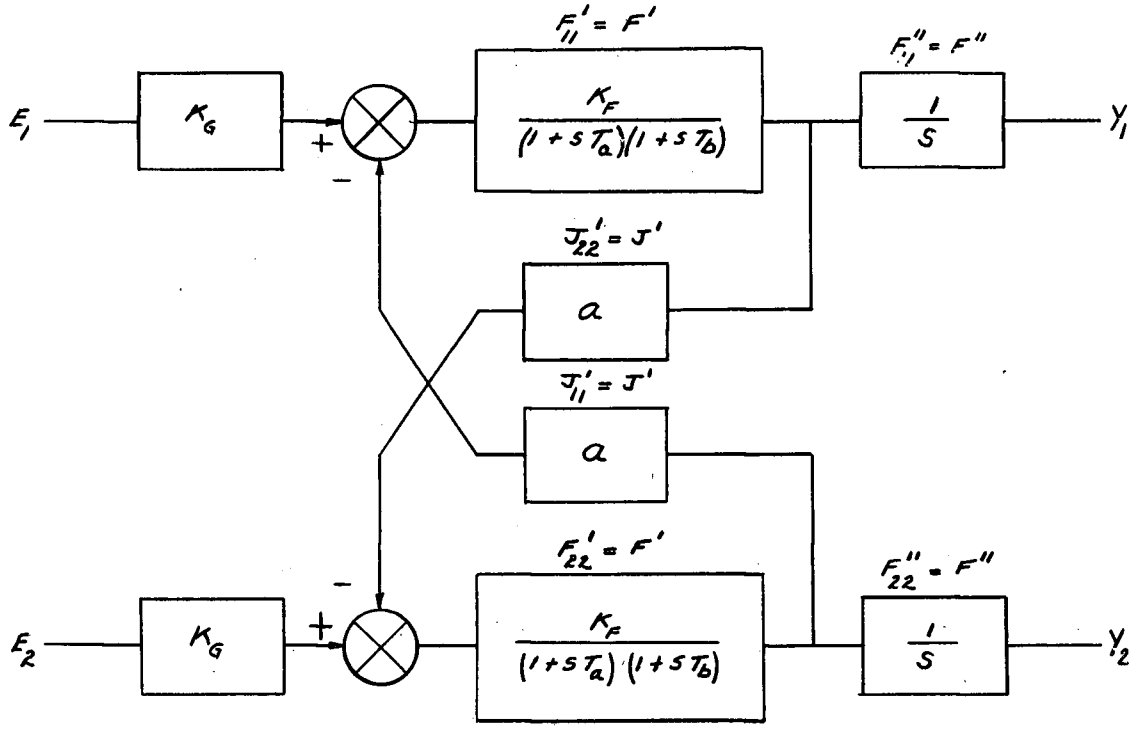

Figure 4-4 Arrangment For Simulation of Two-Axis Tracking System

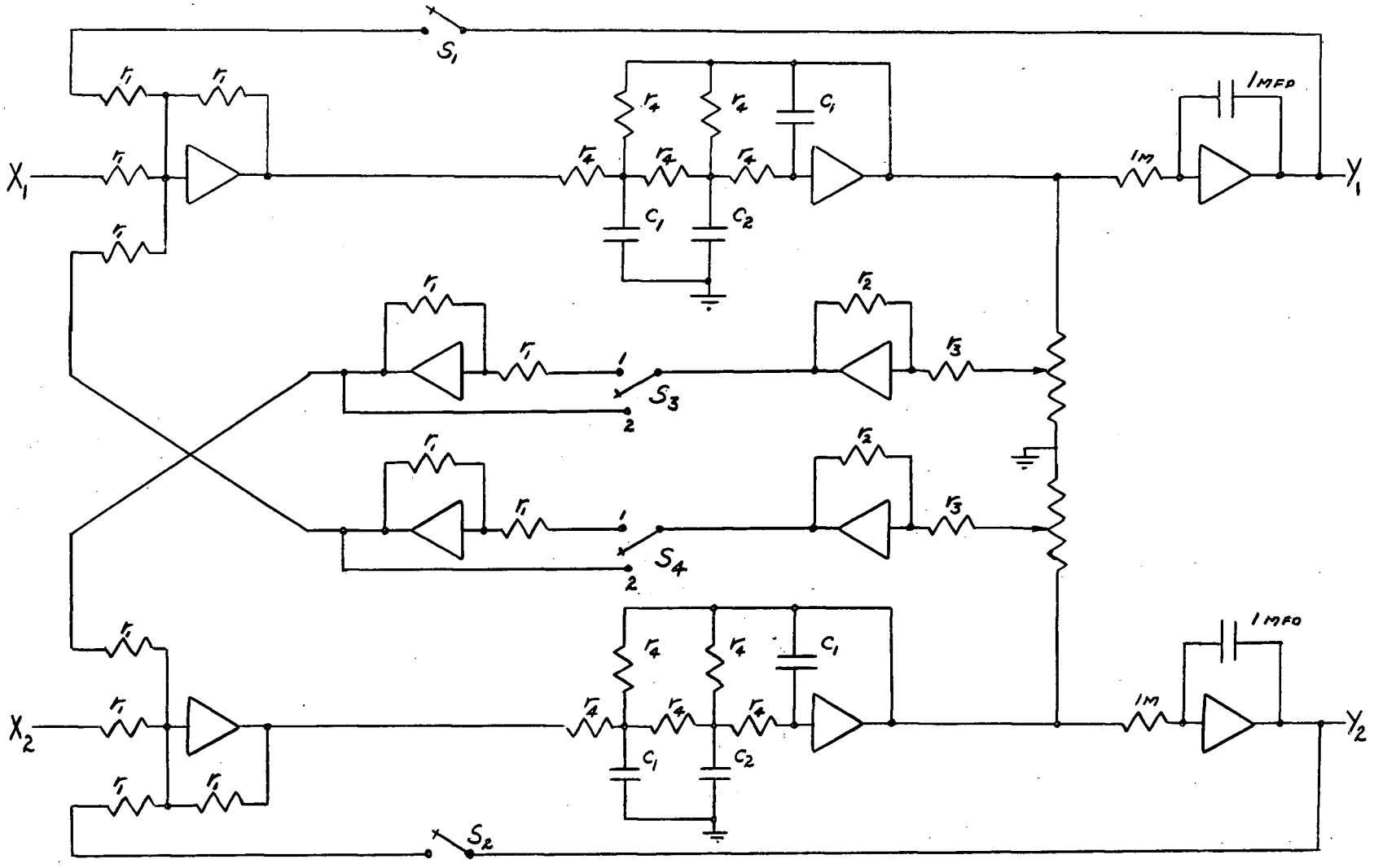

Figure 4-5 Simulation Circuit for Two-Axis Tracking System

$$F' = \frac{1}{3R^2C^2\left(s + \frac{1.09}{2RC}\right)\left(s + \frac{4.91}{2RC}\right)}$$

For the simulation the values

$$R = r_4 = 1 \text{ Meg}$$

$$C = C_1 = 0.1 \ \mu f$$

$$C_2 = 0$$

are chosen. Thus

$$F' = \frac{100/3}{(s + 5.45)(s + 24.55)}$$

From Figure 4-5 we have

$$F'' = \frac{1}{s} \qquad a = \frac{r_2}{r_3}$$

$$G = 1 \qquad c = 1$$

4.4 The Stability of the Open-Loop System

The stability of the open-loop system will be discussed first, i.e., with switches s_1 and s_2 of Figure 4-5 open.

Test 1 - Open-Loop System with Symmetric Cross-Coupling

Switches S_3 and S_4 are in position 1.

Thus $$J'_{11} = J'_{22} = a$$

From equation (4-5) instability occurs when

$$F = \pm \frac{1}{J_{11}J_{22}}$$

or when

$$\frac{100/3}{(s + 5.45)(s + 24.55)} = \frac{\pm 1}{a} \qquad \ldots(4\text{-}12)$$

i.e.,

$$F' = \pm \frac{1}{J'},$$

The left-hand side of equation (4-12) must be entirely real to equal $\frac{\pm 1}{a}$ since a is entirely real. Therefore

$s = j0.$

Now $$F'_{(s=0)} = 0.248$$

Therefore, theoretically the system is unstable when

$$a = \frac{1}{.248} = 4.03$$

Experimental Values

a	System Condition
4.10	stable but highly underdamped
4.125	steady oscillation
4.15	unstable

Comparative Results

	Theoretical	Experimental	% Difference
a	4.03	4.12	2.0

The Nyquist plot of $F'(j\omega)$ is shown in Figure 4-6.

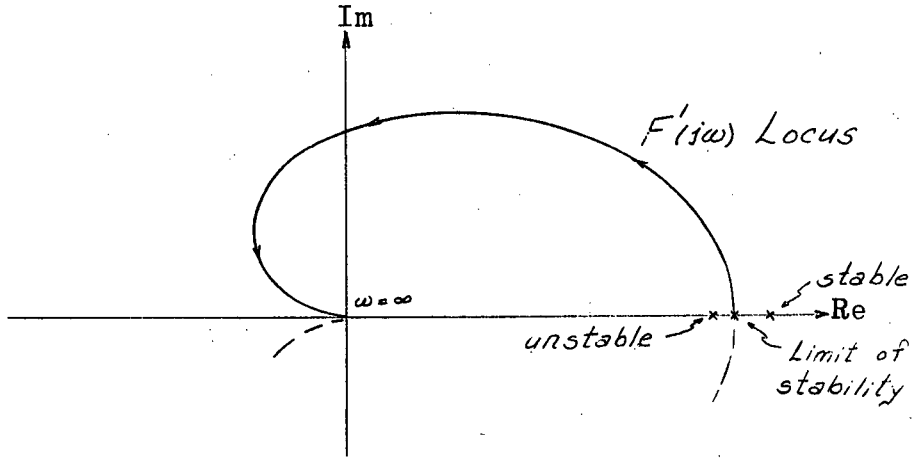

Figure 4-6 Nyquist Plot for Test 1

Test 2 - Open-Loop System with Antisymmetric Cross-Coupling Switch S_3 is in position 1 and switch S_4 is in position 2.

Thus

$$J'_{11} = -J'_{22} = a$$

From equation (4-5) we know that for instability

$$F'(j\omega) = \frac{100/3}{134 - \omega^2 + j30\omega} = \frac{\pm j}{a} \qquad \ldots(4\text{-}13)$$

Now $F'(j\omega)$ must be entirely imaginary to satisfy equation (4-13), therefore

$$\omega_c = \sqrt{134} = 11.6 \text{ rad/sec}$$

Thus

$$F'(j\omega_c) = j0.096$$

Therefore the limit of stability occurs at

$$a = \frac{1}{0.096} = 10.4$$

Experimentally instability occurred at a = 10.4 and $\omega_c = 2\pi \times 1.82 = 11.5$

Comparative Results

	Theoretical	Experimental	% Difference
a	10.4	10.4	0
f	1.84	1.82	1

4.5 The Stability of the Closed-Loop System

The stability of the closed-loop system will now be discussed, i.e., with switches S_1 and S_2 in Figure 4-5 closed.

Test 3 - Closed-Loop System with Symmetric Cross-Coupling Switches S_3 and S_4 are in position 1.

Thus

$$J'_{11} = J'_{22} = a$$

Theoretically instability occurs when (see equation (4-10))

$$as = \pm \frac{s(s + 5.45)(s + 24.55)}{100/3} + 1 \qquad \ldots(4\text{-}14)$$

Experimentally the limit of stability was found at a = 4 and f = .167cps (ω = 1.05). Substituting these values in equation (4-14) gives

$$\text{L.H.S.} = j4.2$$

$$\text{R.H.S.} = j4.18 + .006$$

Thus the experimental results verify equation (4-14). Figure 4-7 shows a Nyquist type plot of the functions of equation (4-14).

Test 4 - Closed-Loop System with Antisymmetric Cross-Coupling

Switch S_3 in position 1; switch S_4 in position 2.

Thus

$$J'_{22} = -J'_{11} = a$$

From equation (4-11), theoretical instability occurs when

$$as = \pm j \frac{s(s + 5.45)(s + 24.55)}{100/3} + 1 \qquad \ldots(4\text{-}15)$$

Experimentally the limit of stability was found at a = 10.4 and f = 1.82cps (ω = 11.5). Substituting these values into equation (4-15) gives

$$\text{L.H.S.} = j119.5$$

$$\text{R.H.S.} = j118.2 + 0.518$$

Thus the experimental results verify equation (4-23). Figure 4-8 shows a Nyquist type plot of the functions of equation (4-15).

When making a Nyquist type plot of the functions of equations (4-14) and (4-15) it is easier to plot the inverse functions. Thus for test 3 we plot

$$\frac{1}{as} \quad \text{and} \quad \frac{\pm 100/3}{s(s + 30s + 134) + 100/3}$$

as shown in Figure 4-7 and for test 4 we plot

$$\frac{1}{as} \text{ and } \frac{\pm j\ 100/3}{s(s + 30s + 134) + 100/3}$$

as shown in Figure 4-8.

Two other tests were conducted, one with

$$J_{11} = \frac{a}{s} \text{ and } J_{22} = a$$

and the other with

$$J_{11} = \frac{a}{s} \text{ and } J_{22} = -a$$

In both these tests the experimental results verified the predicted results.

4.6 Diagonalization of Open-Loop Transfer Matrix

The two-axis tracking system will now be considered using the diagonalization method discussed in chapter 3. The diagonalized system has the form shown in Figure 3-2. From equations (3-19), (3-30) and (3-26a), the desired transfer matrices of the system with antisymmetric cross-coupling i.e., $J_{11} = -J_{22}$, were found to be

$$D = \begin{vmatrix} 1 & -FJ \\ FJ & 1 \end{vmatrix} \qquad F = \begin{vmatrix} F_{11} & 0 \\ 0 & F_{22} \end{vmatrix}$$

$$G = \begin{vmatrix} G_{11} & 0 \\ 0 & G_{22} \end{vmatrix} \qquad C_1 = \begin{vmatrix} 1 & T' \\ T' & 1 \end{vmatrix}$$

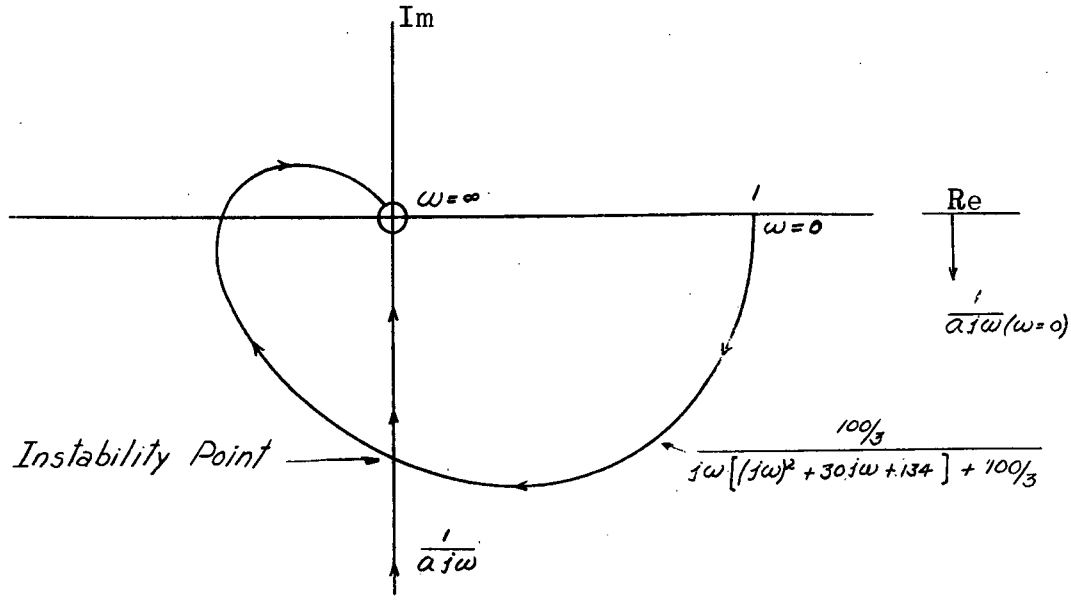

Figure 4-7 Nyquist Plot of Test 3

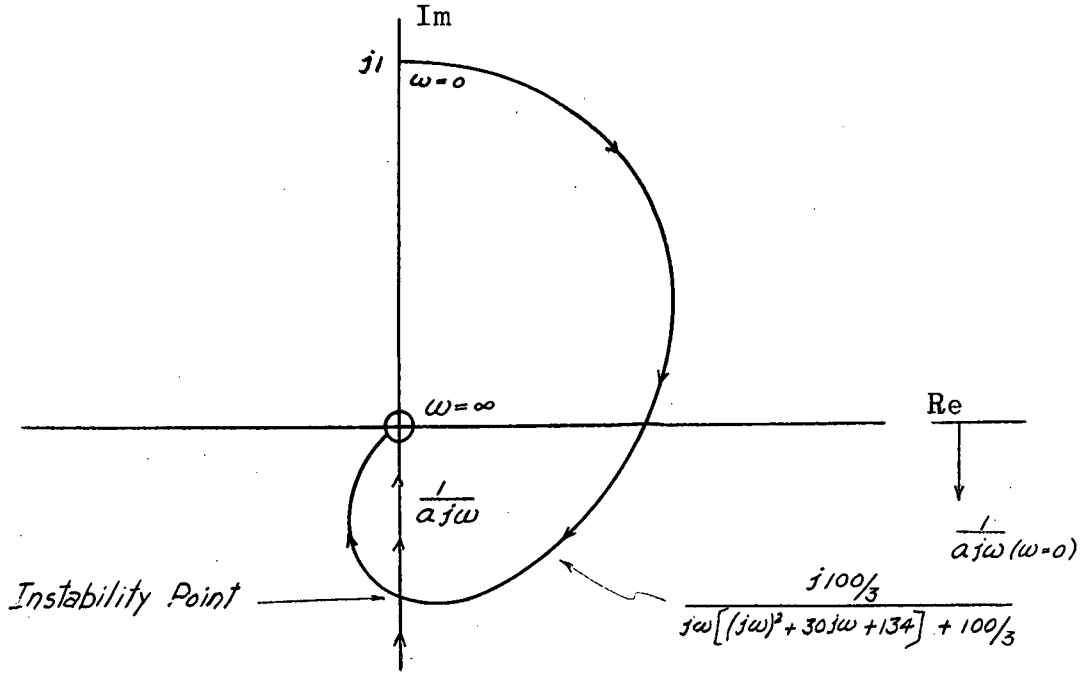

Figure 4-8 Nyquist Plot of Test 4

$$C_2 = (1 + \alpha^2)\begin{pmatrix} C'_{2_{11}} & 0 \\ 0 & C'_{2_{22}} \end{pmatrix}$$

$$T_2 = \frac{1}{1 + \alpha^2}\begin{pmatrix} 1 & -\alpha \\ \alpha & 1 \end{pmatrix}$$

From the first eigenvalue test, equation (4-12), we can obtain

$$JF = \frac{a\ 100/3}{(s + 5.45)(s + 24.55)} \qquad \ldots(4\text{-}16)$$

Substituting this value for JF in equation (3-41) yields

$$T' = \frac{\alpha(s^2 + 30s + 134 - \frac{a\ 100}{3\alpha})}{(s^2 + 30s + 134 + \alpha a\ 100/3)} \qquad \ldots(4\text{-}17)$$

This transfer function can be conveniently realized by means of an active network. This realization is discussed in Appendix II. In order for T' to be realizable in the form given in Appendix II, α must be chosen such that

$$134 - \frac{a\ 100}{3\alpha} > 0$$

or

$$\alpha > \frac{a\ 100}{(3)(134)} \qquad \ldots(4\text{-}18)$$

From the analysis of the system based on the eigenvalue method, we know that the limit of stability was reached at $a = 10.4$ (see Test 4, page 68). At $a = 10.0$ the system was stable but highly underdamped. Suppose that $a = 10.0$

and that the system is to be designed using the diagonalization method. If a = 10.0, we must have

$$a > \frac{1000}{402}$$

$$a > 2.485$$

For the simulation tests α was set at 3.0 and

$$T' = 3\left(\frac{s^2 + 30s + 23}{s^2 + 30s + 1134}\right)$$

was realized by the network shown in Appendix II. Figure 4-9 shows a block diagram of the diagonalized system and Figure 4-10 shows the network analog of the diagonalized two-axis tracking system.

To test the degree of noninteraction achieved by the diagonalization, a fixed sinusoidal signal was applied to an input terminal (say X_1) of both the diagonalized and the undiagonalized system and the amplitude of the outputs was measured. For the undiagonalized case both outputs Y_1 and Y_2 had equal amplitude. For the diagonal system the amplitude of the output Y_2 was approximately 15% of the amplitude of Y_1. Two design criteria were used for comparative tests of the eigenvalue system and the diagonalized system. The criteria are stability and mean-square error. Stability will be discussed first.

4.7 Stability Comparison

Stability was tested by examining the system response to an input wave consisting of a rectangular pulse

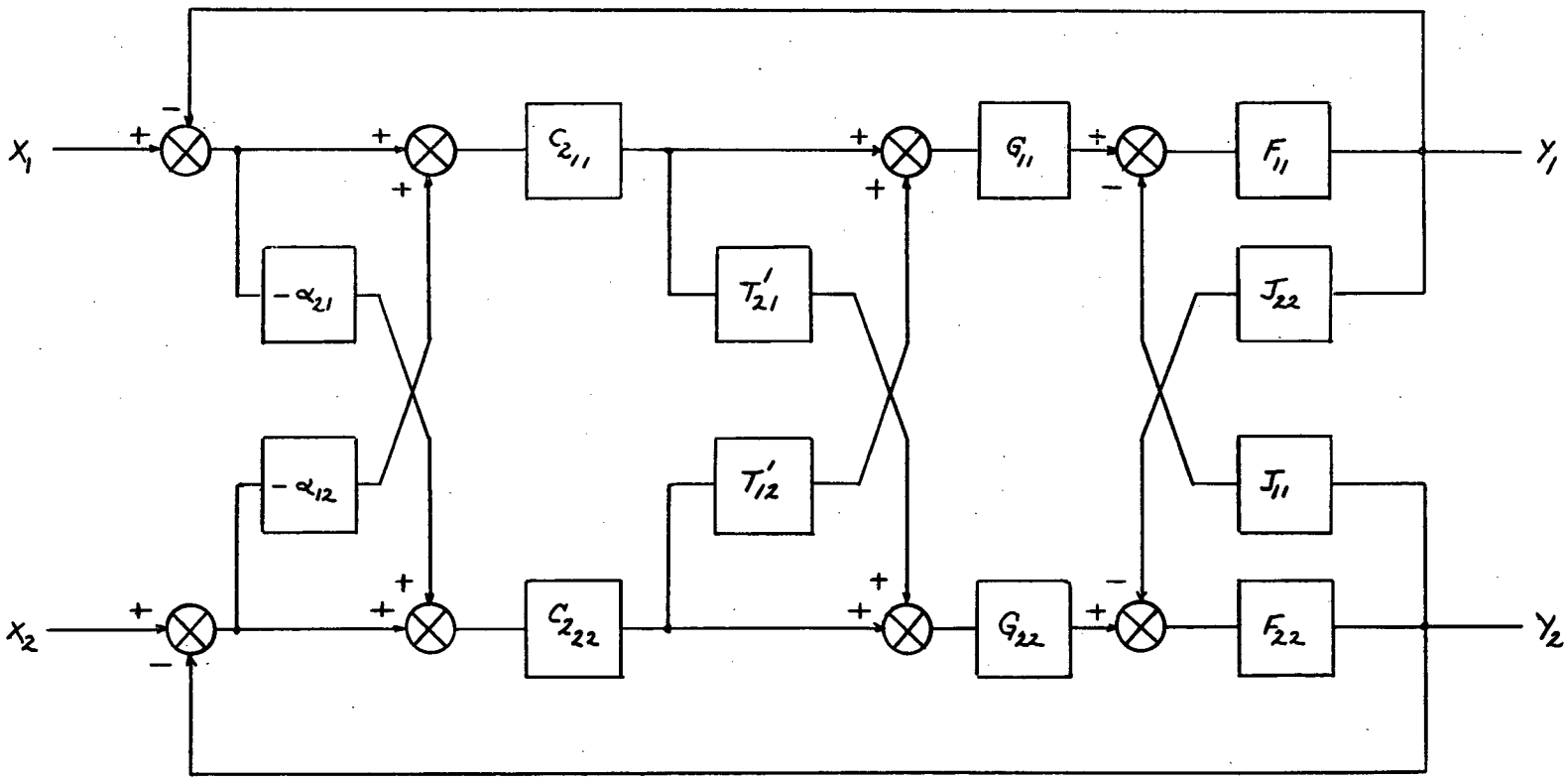

Figure 4-9 Block Diagram of Diagonalized Two-Axis Tracking System

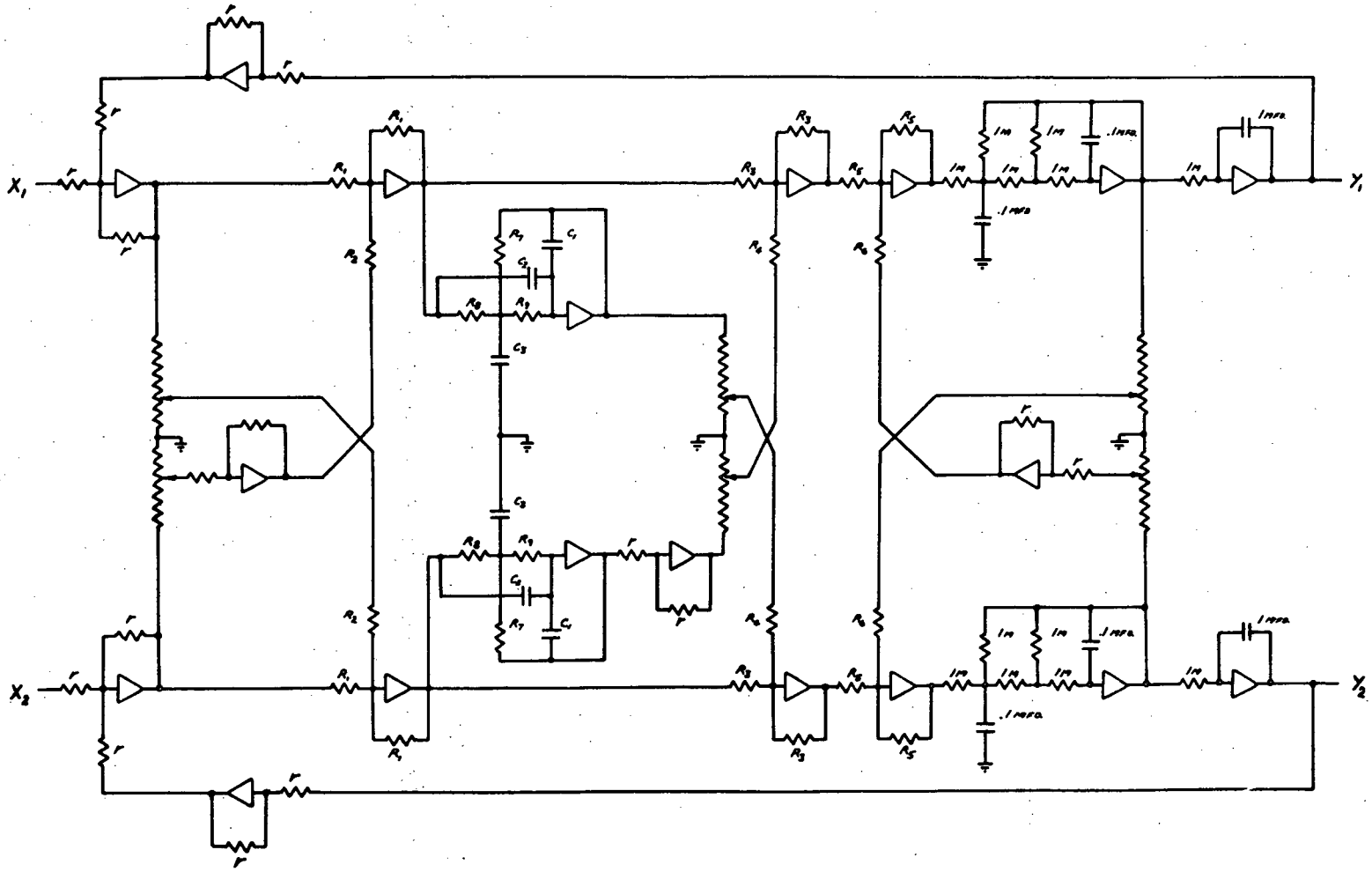

Figure 4-10 Network Analog of the Diagonalized Two-Axis Tracking System

applied manually by a switch. The undiagonalized system was highly underdamped, indicative of its nearly unstable state. The diagonalized system response had approximately a 10% to 15% overshoot and then the oscillation died out very rapidly indicating a stable system. These results are shown in Figures 4-11 and 4-12.

4.8 Mean-Square Error Considerations

In addition to various closed-loop response criteria, one of the most important feedback control systems design criterions is the minimization of the mean-square error. This was the second criterion used for comparative purposes. Consider Figure 4-13

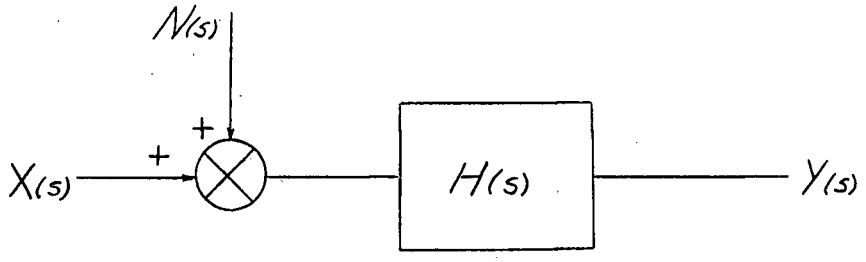

Figure 4-13 System With Noise In Input

Analysis of the system of Figure 4-13 yields

$$Y = H(X + N)$$

For a single-variable system the total mean-square error can be found by the equation

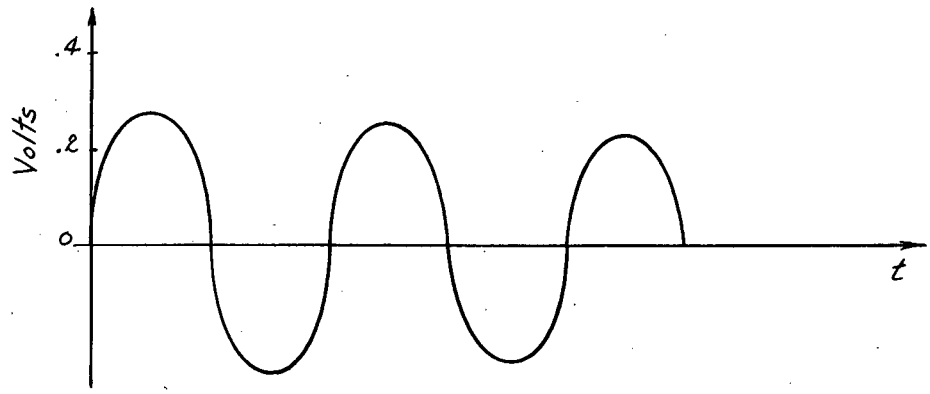

Figure 4-11 Eigenvalue System Response to Single Rectangular Wave Pulse (Very Little Damping)

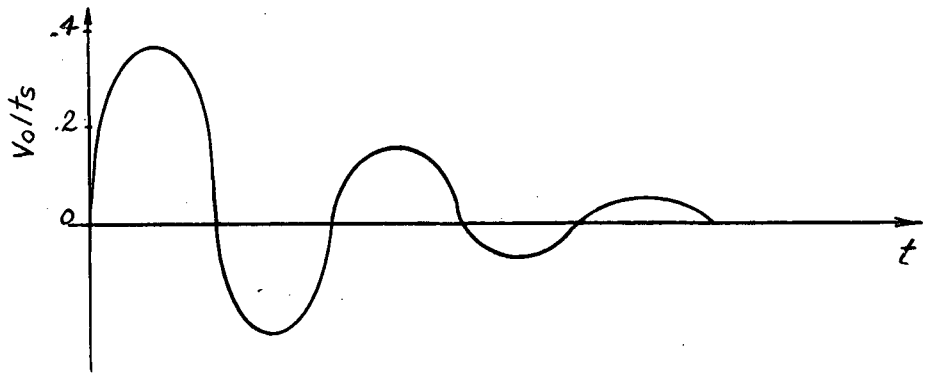

Figure 4-12 Diagonalized System Response to Single Rectangular Wave Pulse (Adequate Damping)

$$\overline{e^2} = \frac{1}{2\pi}\int_{-\infty}^{\infty}\left\{|H(j\omega)|^2\,\Phi_{NN}(j\omega) + |H_d(j\omega) - H(j\omega)|^2\Phi_{XX}(j\omega)\right\}d\omega \qquad \ldots(4\text{-}19)$$

where

$H(j\omega)$ = system transfer function

$\Phi_{NN}(j\omega)$ = Noise auto-correlation function

$\Phi_{XX}(j\omega)$ = Signal auto-correlation function

$H_d(j\omega)$ = desired system transfer function

If we are concerned with an input signal which is entirely noise, equation (4-19) reduces to

$$\overline{e^2} = \frac{1}{2\pi}\int_{-\infty}^{\infty}|H(j\omega)|^2\,\Phi_{NN}(j\omega)d\omega \qquad \ldots(4\text{-}20)$$

It is apparent that, for a multivariable system, to apply this equation in matrix form and solve for

$$\overline{e^2} = e_1^2 = e_1^2 + e_2^2 + \ldots\ldots e_n^2 \qquad \ldots(4\text{-}21)$$

would involve a great deal of labour. If a system is at all complicated, the most realistic method for determing the optimum choice of parameters for a fixed configuration is by experimental determination of e^2. This is done quite simply in the manner shown in Figure 4-14.

This type of procedure was applied to both the diagonalized and undiagonalized systems. A random signal

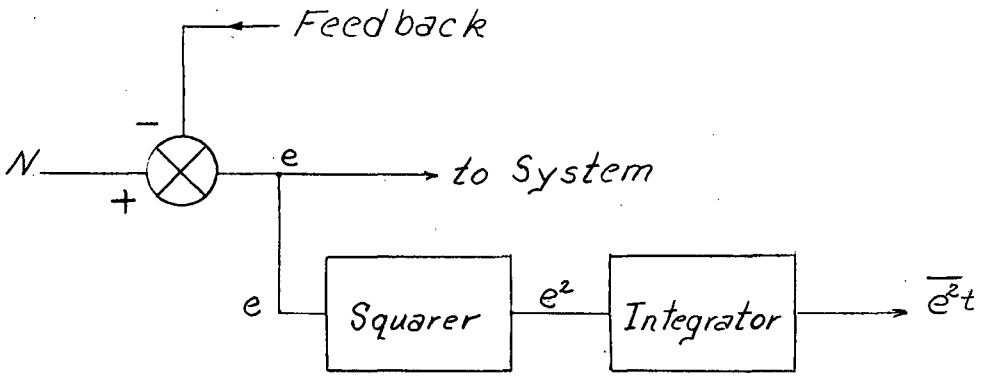

Figure 4-14 Experimental Determination of $\overline{e^2}$

with a white noise output in the range 0.04 cps to 10 cps was introduced at X_1 and e_1^2 and e_2^2 were measured and recorded. This was also done for the signal introduced at X_2. The parameter α representing the gain of the cross-coupling elements was varied. The results of these tests are shown in Figures 4-15 and 4-16.

From Figures 4-15 and 4-16 we can see the mean-square error remains relatively flat (within the accuracy of the experiment) as the degree of cross-coupling is varied for both the diagonalized and the undiagonalized systems. Consequently in this particular case a mathematical analysis to determine $\overline{e^2}$ would be fruitless since it is evident that the minimum mean-square error (with respect to α) criterion does not have any significance.

4.9 Comparative Comments

It is seen that in the case considered the

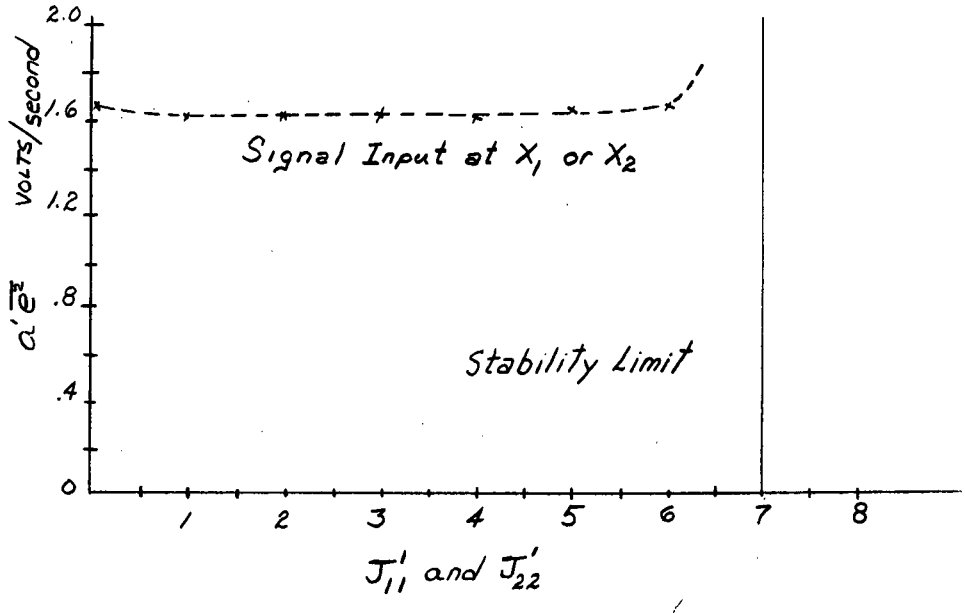

Figure 4-15 Eigenvalue System Mean-Square Error

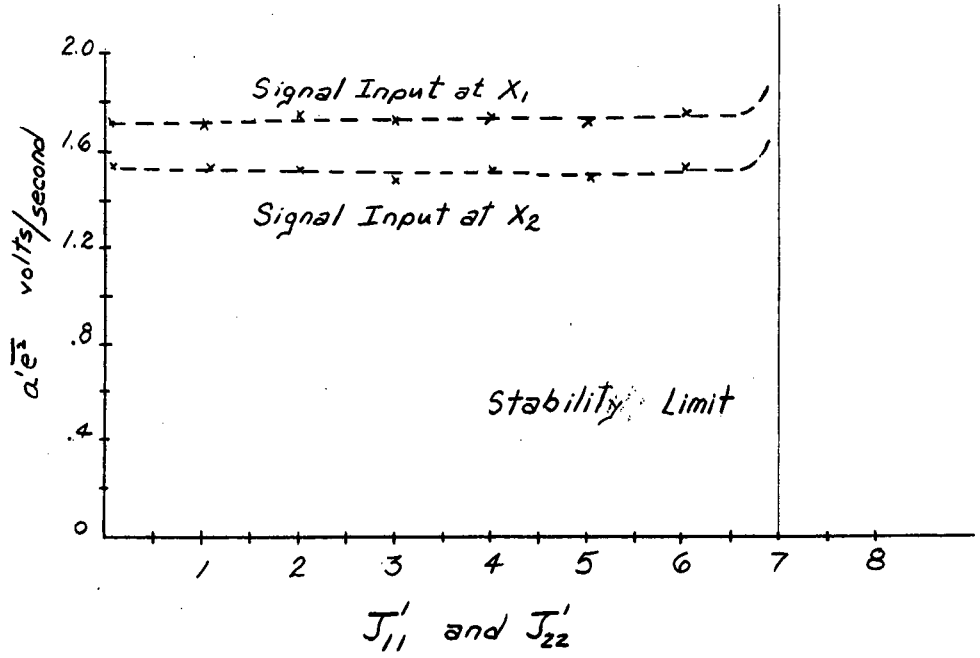

Figure 4-16 Diagonalized System Mean-Square Error

diagonalized system is more stable than the eigenvalue system, since with a = 10.0 the latter was near the limit of stability while the stability margin of the former was adequate.

The mean-square error tests did not show one system to be superior to the other.

In both systems, i.e., the eigenvalue and the diagonalized, no compensating networks have been used to improve system performance. If such networks were desirable, it would be simpler to deal with the diagonalized system. Consider the s-plane Figures 4-17 and 4-18. It is quite apparent that to compensate $G_c(j\omega)$ in Figure 4-17 so that the $G_c(j\omega)$ locus avoids the $\lambda_k(j\omega)$ locus would be considerably more difficult than to compensate $B_{kk}(j\omega)$ in Figure 4-18 so that the $B_{kk}(j\omega)$ locus does not encircle the -1 point.

Considerably more elements are required in a diagonalized system (approximately twice as many). To reduce the number of components required it may be possible to achieve approximate noninteraction by approximating the transfer functions using simple RC networks. For example

$$T'' = \frac{s^2 + 30s + 23}{s^2 + 30s + 1134}$$

can be very crudely approximated by the network shown in Figure 4-19.

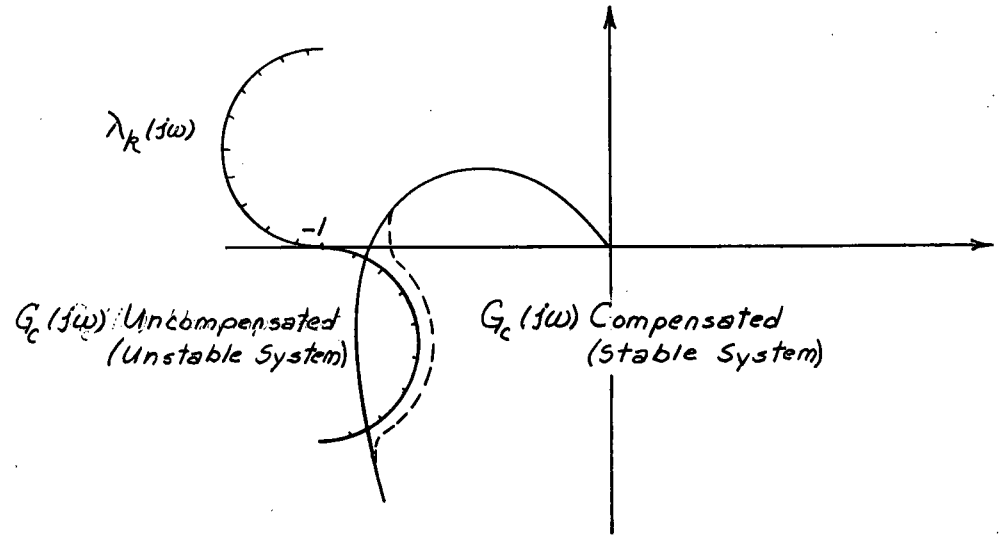

Figure 4-17 Eigenvalue System Compensation

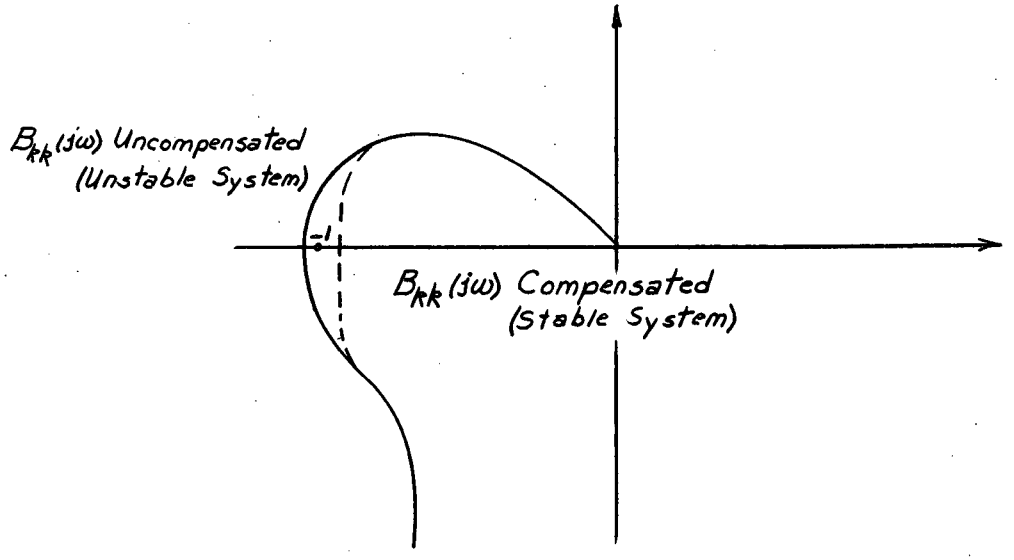

Figure 4-18 Diagonalized System Compensation

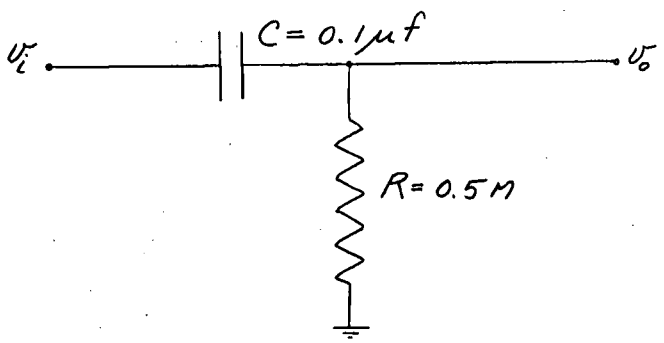

Figure 4-19 Approximate T" Network

Using this particular network in the system the same tests as before were carried out. The results of these tests were:

(1) Diagonalization was nearly nonexistent, i.e., interaction was very strong.

(2) Response to a single square wave pulse was somewhat better than the eigenvalue system. Overshoot was approximately the same as with the active network (10-15%) but the oscillations took approximately 5 times longer to damp out.

(3) The mean-square error stayed relatively flat as the cross-coupling was varied, however, the value of $\overline{e^2}$ was approximately twice that of the "active network" system.

The unsatisfactory results from this transfer function approximation is probably due to the fact that the approximation is inadequate over a sufficient bandwidth.

5. EIGENVALUE METHOD APPLIED TO A STABILITY STUDY OF FOUR PARALLEL CONNECTED SYNCHRONOUS MACHINES

The following is an example of the eigenvalue method as applied to a system of four parallel connected synchronous machines.

The block diagram for incremental operation is shown in Figure 5-1 where

$G_p = s(M_1 s + 1)$ = transfer function of the prime mover

$G_T = \dfrac{1}{(1 + sT_1)(1 + sT_2)}$ = transfer function of torque producing element

$G_c = \dfrac{1}{s(1 + sT_3)}$ = compensating network

sD_i = Laplace transform of incremental speed deviation

T_{ki} = synchronizing torque coefficient of k^{th} and i^{th} lines

L_i = local load disturbance

This is a four generator system and all the generators and control elements are assumed to have identical transfer functions. This is not a restriction; it merely simplifies the procedure for illustrating the principle involved. This system can be analyzed using the eigenvalue method.

Analysis of the single loop shown in Figure 5-1 yields

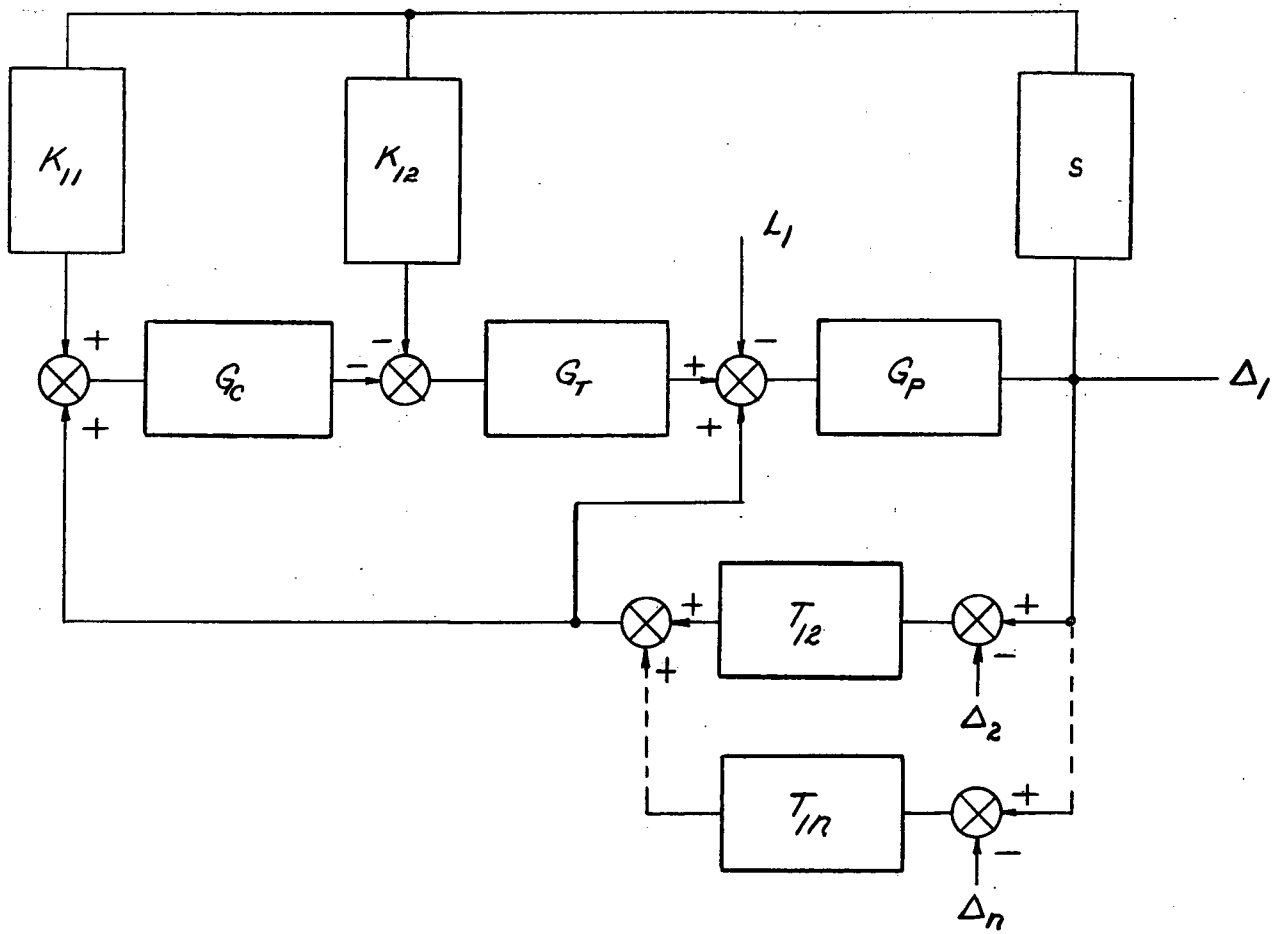

Figure 5-1 Single-Loop of Parallel Operated Synchronous Machines

$$\left(\frac{1}{G_p} + sG_T(K_{11}G_c + K_{12}) + (1 + G_cG_T) \sum_{k=2}^{n} T_{1k}\right)\Delta_1$$

$$- (1 + G_cG_T) \sum_{k=2}^{n} T_{1k} = L_1 \qquad \ldots(5\text{-}1)$$

Now setting

$$-\lambda = \frac{1}{G} = \frac{\frac{1}{G_p} + sG_T(K_{11}G_c + K_{12})}{1 + G_cG_T} \qquad \ldots(5\text{-}2)$$

and writing equation (5-1) in general form gives

$$(-\lambda + \sum_{1}^{n} T_{ik})\Delta_i - \sum_{1}^{n} T_{ik}\Delta_k = \frac{-L_i}{1 + G_cG_T} \qquad \ldots(5\text{-}3)$$

where $i = 1,2 \ldots .n$

$k = 1,2 \ldots .n$

$i \neq k$

Let

$$A_{mm} = \sum_{1}^{n} T_{mk}$$

$$m \neq k \qquad \ldots(5\text{-}4)$$

$$A_{mk} = -T_{mk}$$

be the elements of the matrix A.

System stability can be determined from a Nyquist plot of the function

$$R_k(s) = \frac{1}{\lambda_k(s)} + G \qquad \ldots(5\text{-}5)$$

where the λ_k's are the eigenvalues of the matrix A.

Such a system has been dealt with by Crary[12]. A network analyzer was used to determine the synchronizing coefficients T_{jk} and the swing curves evaluated by numerical integration.

The following discussion will deal with the stability of the linearized system under various possible network conditions. From equations (5-4) we obtain the eigenvalue equation

$$\begin{vmatrix} -\lambda + T_{11} & -T_{12} & -T_{13} & -T_{14} \\ -T_{21} & -\lambda + T_{22} & -T_{23} & -T_{24} \\ -T_{31} & -T_{32} & -\lambda + T_{33} & -T_{34} \\ -T_{41} & -T_{42} & -T_{43} & -\lambda + T_{44} \end{vmatrix} = 0 \qquad \ldots(5\text{-}6)$$

where

$$T_{kk} = \sum_{\substack{j=1 \\ j \neq k}}^{4} T_{kj}$$

To illustrate the applicability of the eigenvalue method, let us use the tie-line coefficients given by Crary. Since we are dealing with the stability for the linearized system, we shall neglect the intial incremental deviations in angular displacement and the power angles.

It is apparent from equation (5-7) that one λ value is going to be zero. This is seen by adding the second, third and fourth columns to the first.

Using Crary's values for the synchronizing coefficients the following determinants were solved on the Alwac III E digital computer:

(1) Fault On

$$\begin{vmatrix} -\lambda + .7931 & -.7480 & -.0231 & -.0220 \\ -.7480 & -\lambda + 1.0440 & -.1510 & -.1450 \\ -.0231 & -.1510 & -\lambda + .2378 & -.0638 \\ -.0220 & -.1450 & -.0638 & -\lambda + .2307 \end{vmatrix} = 0$$

(2) Fault Partially Cleared

$$\begin{vmatrix} -\lambda + .863 & -.782 & -.038 & -.043 \\ -.782 & -\lambda + 1.311 & -.250 & -.279 \\ -.038 & -.250 & -\lambda + .413 & -.125 \\ -.043 & -.279 & -.0638 & -\lambda + .447 \end{vmatrix} = 0$$

(3) Fault Cleared

$$\begin{vmatrix} -\lambda + 1.205 & -.960 & -.116 & -.129 \\ -.960 & -\lambda + 2.567 & -.760 & -.847 \\ -.116 & -.760 & -\lambda + 1.247 & -.371 \\ -.129 & -.847 & -.371 & -\lambda + 1.347 \end{vmatrix} = 0$$

The eigenvalues for these determinants are given in table 5.1.

System Condition	Eigenvalues λ_1	λ_2	λ_3	λ_4
Fault On	0	1.689	.318	.29
Fault Partially Cleared	0	1.936	.559	.513
Fault Cleared	0	3.424	1.69	1.251

Table 5.1 Eigenvalues

Essentially we have reduced the multivariable system of Figure 5-1 to four equivalent single variable systems as shown in Figure 5-2.

5.1 Nyquist Stability Investigation

Now to graphically study the stability of the system, we construct a Nyquist plot of the function

$$R_k(s) = \frac{+1}{\lambda_k} + G(s)$$

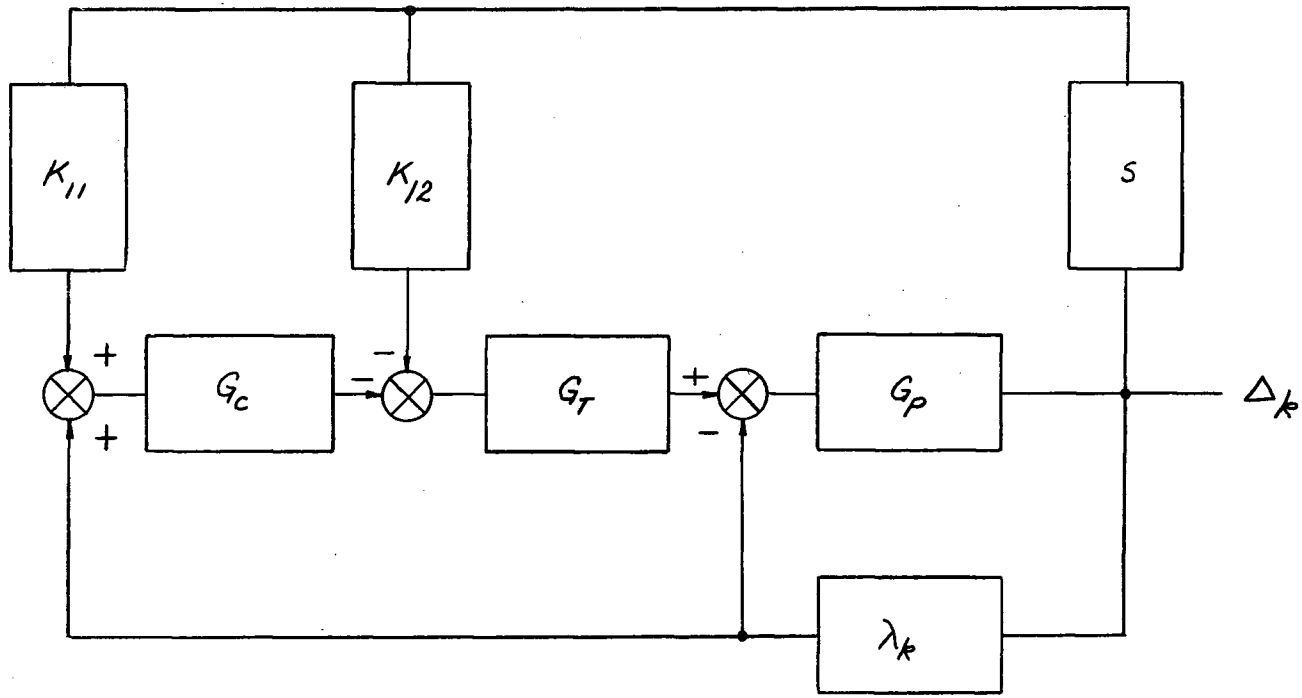

Figure 5-2 Equivalent Multi-Loop Single Variable System

Substitution of the proper transfer functions into equation (5-2) yields

$$G(s) = \frac{\left[s(1+T_1s)(1+T_2s)(1+T_3s)+1\right](1+M_1s)}{(1+T_1s)(1+T_2s)(1+T_3s)+s(1+M_1s)(K_{11}+K_{12}s(1+T_3s))}$$

To plot the function G(s), we consider the behaviour of the function as $s \to 0$ and as $s \to \infty$. We find that

$$G(s) \underset{(s \to \infty)}{\Rightarrow} \frac{T_1T_2s}{K_{12}}$$

$$G(s) \underset{(s \to 0)}{\Rightarrow} 1$$

Knowing the necessary time constants and gains we can then plot the G(s) locus.

In the case considered, suppose the G(s) locus is as shown in Figure 5-3. From Figure 5-3 we know that the system will be unstable if the $G(j\omega)$ locus intersects or encloses the critical points $-\frac{1}{\lambda_k}$ $(k = 1,2,3,4)$.

5.1 Root-Loci Stability Investigation.

Another way to graphically study the stability of the system is to determine a root-locus plot of the function $\lambda_k G$.

Suppose we consider the root-locus plot of the

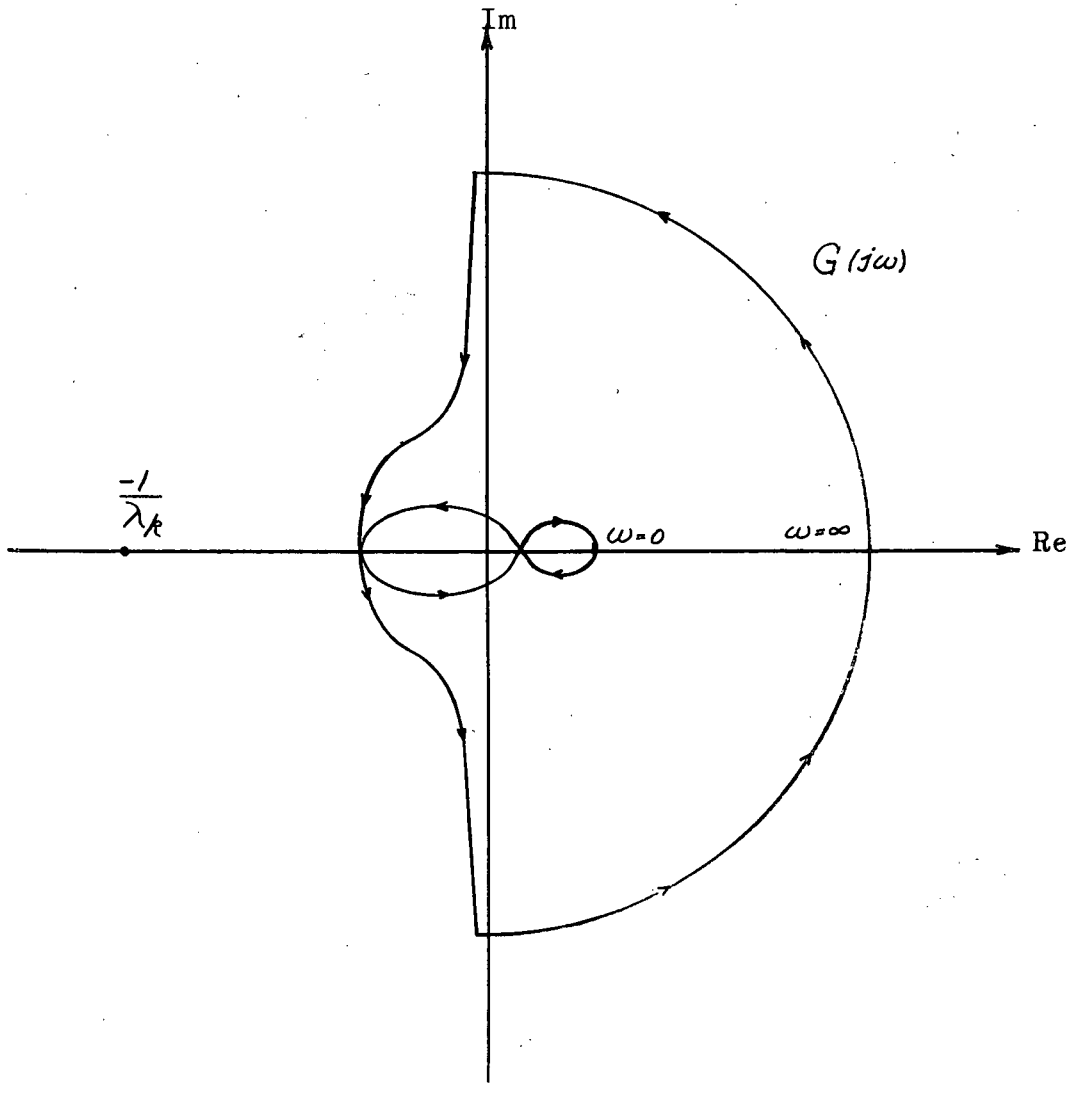

Figure 5-3 Nyquist Plot of $R_k(j\omega) = \frac{+1}{\lambda_k} + G(j\omega)$

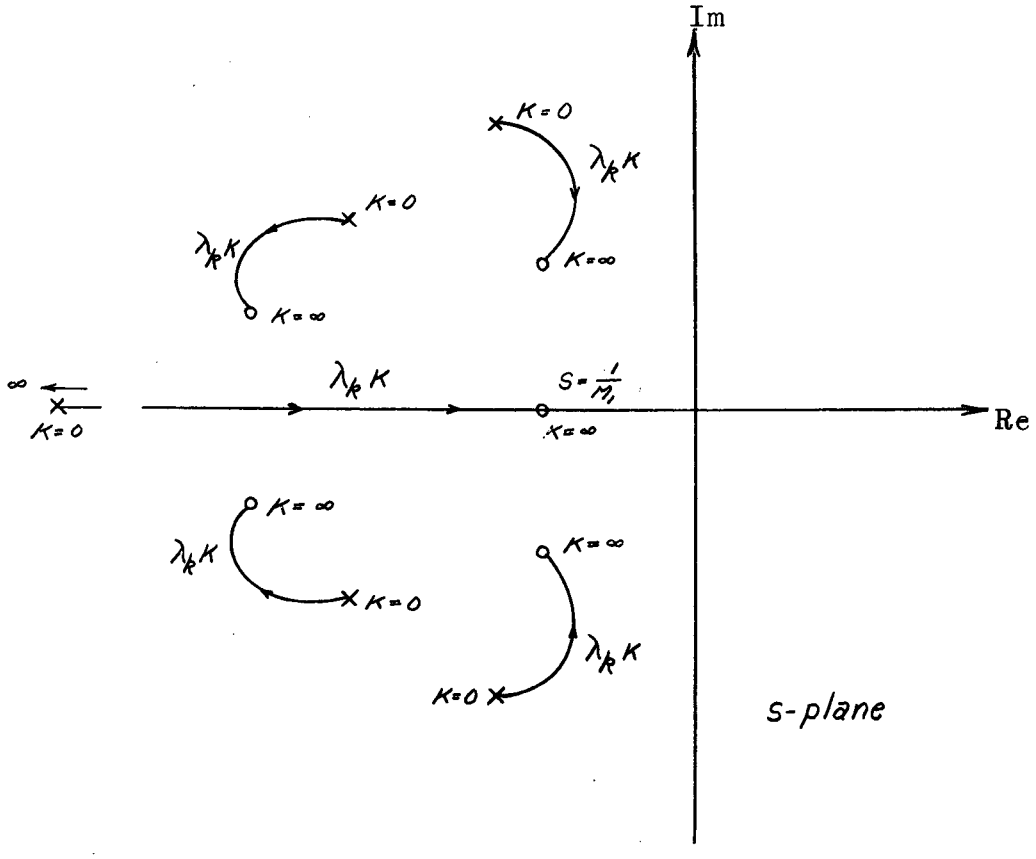

Figure 5-4 Root-Locus Plot of the Function $\lambda_k K$

function KG where K is variable from 0 to ∞ . A root-locus plot of KG can then take the form shown in Figure 5-4. The system will remain stable provided that the root-loci remain in the left-half s-plane.

One such diagram is sufficient for a complete root-locus analysis of the system. The roots are found by locating the value of $K = \lambda_k$, for example the condition $K = 0$ gives the roots for $\lambda = 0$ as shown in Figure 5-4. For different network conditions the λ_k's change. The corresponding locations of the characteristic roots in the s-plane can be determined from Figure 5-4.

If a root-locus analysis of the characteristic equation of the system is attempted by conventional methods, a polynomial with 20 zeros would have to be considered and considerably more labour would be involved. Thus it is apparent that the eigenvalue method provides a simpler root-locus analysis for this system.

6. CONCLUSION

Single variable graphical analysis and design techniques have been shown to be applicable to certain types of multivariable systems when the eigenvalue method and the diagonalized method are used. The experimental determination of system eigenvalues has been investigated and shown to be feasible. The suitability of simulation studies to verify design, to investigate the influence of parameter variations and to evaluate the mean-square error has been shown.

A comparison of the eigenvalue method and the more complicated diagonalization method has been made. It was seen that the design methods are very useful to determine initial system configuration for simulation studies. The simulated system can then be used to perform optimization and further improvements.

The eigenvalue method has been applied to a system of four parallel-connected synchronous generators and graphical methods of stability investigation have been discussed.

Appendix I

Consider the network shown in Figure AI-1

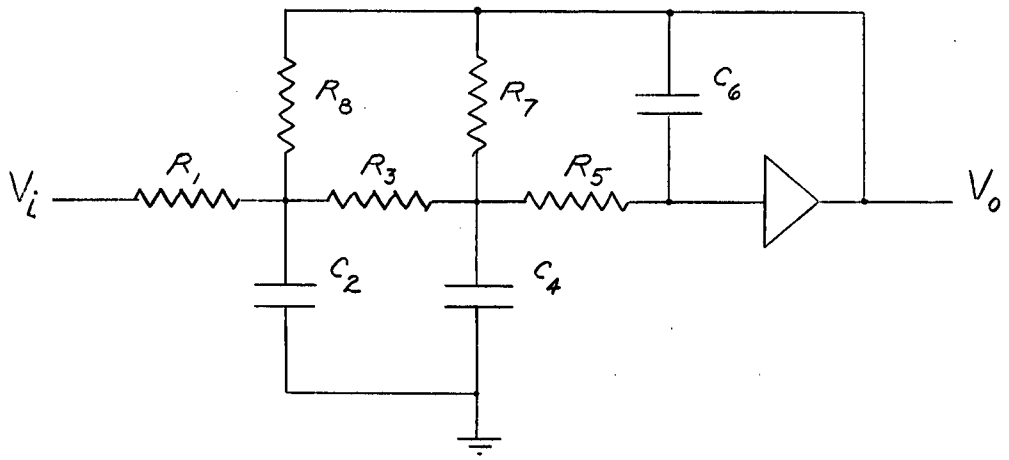

Figure AI-1

Wadhwa[13] has shown this network to have the transfer function

$$\frac{V_0}{V_i} = \frac{-b_0}{a_3 s^3 + a_2 s^2 + a_1 s + 1} \qquad \ldots(AI-1)$$

where

$$b_0 = \frac{\alpha^2}{(1 + 3\alpha)}$$

$$a_1 = \frac{\alpha}{(1 + 3\alpha)} RC_2 + (1 + \alpha)RC_6$$

$$a_2 = \frac{\alpha(1 + 2\alpha)}{(1 + 3\alpha)} R^2C_6(C_2 + C_4)$$

$$a_3 = \frac{\alpha^2}{(1 + 3\alpha)} R^3 C_2 C_4 C_6$$

$$R_1 = R_3 = R_5 = R \qquad R_7 = R_8 = \alpha R$$

$$a_1 > \frac{a_3(1 + 2\alpha)}{a_2(1 + 3\alpha)}$$

Now setting $C_4 = 0$ makes $a_3 = 0$

If we set $\alpha = 1$

$$C_2 = C_6 = C$$

equation AI-1 becomes

$$\frac{V_0}{V_i} = \frac{1}{3R^2C^2\left(s + \frac{1.09}{2RC}\right)\left(s + \frac{4.91}{2RC}\right)} \qquad \ldots(AI-2)$$

Appendix II

Consider the network configuration shown in Figure AII-1

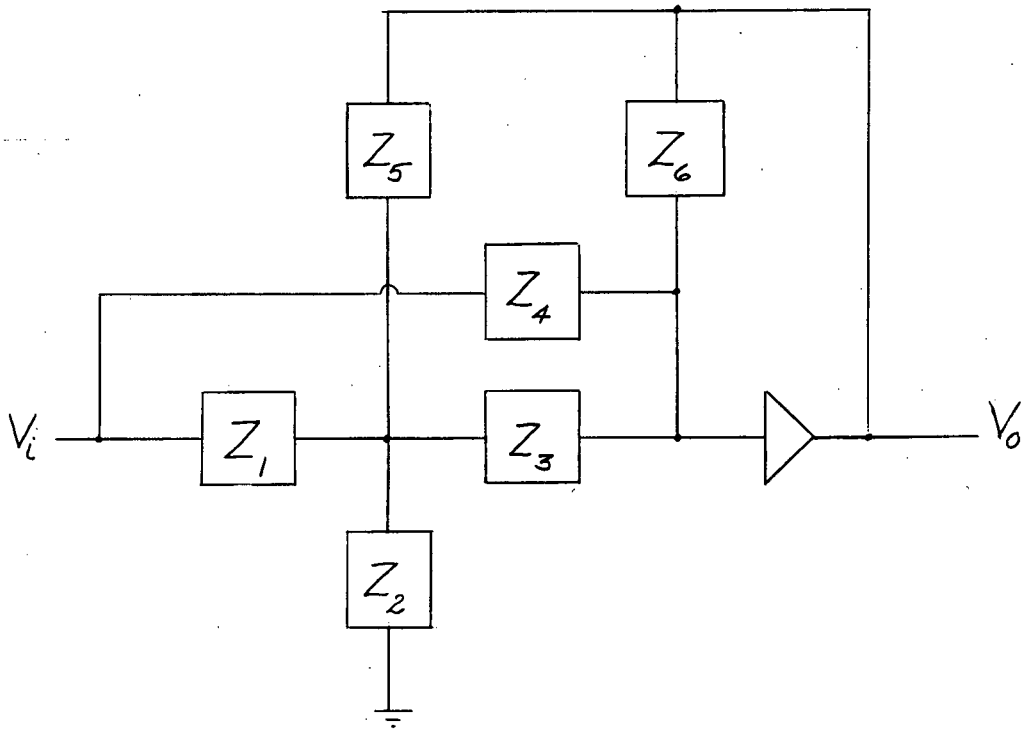

Figure AII-1

The transfer function has the form

$$\frac{V_0}{V_i} = - \frac{\frac{1}{Z_1} + \frac{Z_3}{Z_4}\left(\frac{1}{Z_1} + \frac{1}{Z_2} + \frac{1}{Z_3} + \frac{1}{Z_5}\right)}{\frac{1}{Z_5} + \frac{Z_3}{Z_6}\left(\frac{1}{Z_1} + \frac{1}{Z_2} + \frac{1}{Z_3} + \frac{1}{Z_5}\right)} \quad \ldots(\text{AII-1})$$

Now if we set

$$\frac{1}{Z_1} = \frac{1}{R_1} \qquad \frac{1}{Z_2} = C_2 s$$

$$\frac{1}{Z_3} = \frac{1}{R_3} \qquad \frac{1}{Z_4} = C_2 s$$

$$\frac{1}{Z_5} = \frac{1}{R_5} \qquad \frac{1}{Z_6} = C_6 s$$

Substituting these values into equation AII-1 yields

$$\frac{V_0}{V_i} = - \frac{s^2(C_2R_3C_4) + sR_3C_4(\frac{1}{R_1} + \frac{1}{R_3} + \frac{1}{R_5}) + \frac{1}{R_1}}{s^2(C_2R_3C_6) + sR_3C_6(\frac{1}{R_1} + \frac{1}{R_3} + \frac{1}{R_5}) + \frac{1}{R_5}}$$

Now if $C_4 = C_6$ we obtain

$$\frac{V_0}{V_i} = - \frac{s^2 + s\frac{1}{C_2}(\frac{1}{R_1} + \frac{1}{R_3} + \frac{1}{R_5}) + \frac{1}{R_1R_3C_2C_4}}{s^2 + s\frac{1}{C_2}(\frac{1}{R_1} + \frac{1}{R_3} + \frac{1}{R_5}) + \frac{1}{R_5R_3C_2C_6}} \quad \text{...(AII-2)}$$

REFERENCES

1. Povejail, D.J. and Fuchs, A.M., "A Method for the Preliminary Synthesis of Complex Multi-Loop Control Systems", Trans. AIEE, Pt. 2, Vol. 74, pp. 129-134, July, 1955.

2. Kavanagh, R.J., "Multivariable Control Systems Synthesis", Trans. AIEE, Pt. 2, Vol. 77, pp. 425-429, November, 1958.

3. Freeman, H., "A Synthesis Method of Multipole Control Systems", Trans. AIEE, Pt. 2, Vol. 76, pp. 28-31, March, 1957.

4. Horowitz, I.M., "Synthesis of Linear Multivariable Feedback Control Systems", IRE Trans., PGAC, Vol. AC-5, pp. 94-105, June, 1960.

5. Hsieh, H.C., and Leondes, C.T., "On the Optimum Synthesis of Multipole Control Systems in the Wiener Sense", IRE National Convention, March, 1959.

6. Krasovskii, A.A., "Two Channel Automatic Regulation Systems with Antisymmetric Crosso Connections", Automation and Remote Control, Pt. 2, Vol. 18, pp. 139-149, February, 1957.

7. Newman, D.B., "The Analysis of Cross-Coupling Effects on the Stability of Two-Dimensional, Orthogonal, Feedback Control Systems", IRE Trans., PGAC, Vol. AC-5, pp. 314-320, September, 1960.

8. Bohn, E.V., "Design and Synthesis Methods for a Class of Multivariable Feedback Control Systems Based on Single-Variable Methods", Trans. AIEE, paper No. 62-75, December, 1961.

9. Bohn, E.V., "Stabilization of Linear Multivariable Feedback Control Systems", Trans. IRE, September, 1960, pp. 321-322.

10. Boksenbom, A., and Hood, R., "General Algebraic Method Applied to Control Analysis of Complex Engine Types", Natl. Advisory Committee for Aeronautics, Washington, D.C., Rept. No. 980, April, 1959.

11. Meerov, M.V., "The Autonomy of Multi-Loop Systems Which are Stable When Their Steady-State Precision is Increased Without Limit", Automation and Remote Control, No. 5, pp. 411-424, 1956.

12. Crary, J.B., Power System Stability, John Wiley and Sons, New York, Vol. II, Chapter 5, Sections 18 and 19, 1945.

13. Wadhwa, L.K., "Simulation of Third-Order System with One Operational Amplifier", Proc. IRE, pp. 201-202, February, 1960.

14. Kavanagh, R.J., "Noninteracting Controls in Linear Multivariable Systems", Trans. AIEE, Pt. 2, Vol. 76, pp. 95-99, May, 1957.

15. Freeman, H., "Stability and Physical Realizability Consideration in the Synthesis of Multipole Control Systems", Trans. AIEE, Pt. 2, Vol. 77, Applications Industry, pp. 1-5, March, 1958.

16. Bohn, E.V., and Kasvand, T., "The Use of Matrix Transformations and System Eigenvalues in the Design of Linear Multivariable Control Systems", (to be Published).

17. Truxal, J.G., Control Systems Synthesis , McGraw-Hill, New York, pp. 454-457, 1955.

18. Kirchmayer, L.K., "Differential Analyzer Aids Dispatching System Design", Trans. AIEE, Pt. 2, Vol. 75, pp. 572-579, January, 1959.

19. Mesarovic, M.D., The Control of Multivariable Systems, The Technology Press, Cambridge, Massachusetts and New York, Wiley and Sons, 1960.